GAMMA AND NEUTRON DOSE PROFILES NEAR A CF-252 BRACHYTHERAPY SOURCE

A Thesis
Presented to
The Academic Faculty

By

Eugene C. Fortune IV

Partial Fulfillment
Of the Requirements for the Degree
Master of Science in Nuclear and Radiological Engineering

Georgia Institute of Technology

August 2010

GAMMA AND NEUTRON DOSE PROFILES NEAR A CF-252 BRACHYTHERAPY SOURCE

Approved by:

Dr. C-K. Chris Wang, Advisor
Nuclear and Radiological Engineering
Georgia Institute of Technology

Dr. Sang Hyun Cho
Nuclear and Radiological Engineering
Georgia Institute of Technology

Ian C. Gauld
Nuclear Science and Technology Division
Oak Ridge National Laboratory

Date Approved: June 29, 2010

Acknowledgements

First I would like to thank Jesus Christ my Lord and Savior through which all things are possible. Thanks to my parents whose love and support have allowed me to reach this point in my life.

A special thanks to Dr. C-K Chris Wang and Ian C. Gauld who were with me every step of the way through my research, computational modeling, experimenting, and writing. Their help and guidance allowed me to conduct this study efficiently and successfully. I would like to thank Dr. Sang Cho for taking the time to serve on my thesis committee.

Thanks to Dr. Nolan Hertel for allowing me to use his electrometer to perform my experiment as part of this study and Eric Burgett for taking the time to assist me with the experimental setup and implementation.

I owe a special thanks to Dr. Bruce Patton at Oak Ridge National Laboratory (ORNL) for assisting me with my MCNP computational models while I was at ORNL.

Thanks to Christina Tabor and the Georgia Tech Office of Radiological Safety for their guidance and supervision during the experiment to make sure everything was done safely.

Table of Contents

List of Tables

List of Figures

Summary

A new generation of medical grade ^{252}Cf sources was developed in 2002 at the Oak Ridge National Laboratory (ORNL). The combination of small size and large activity of these ^{252}Cf sources makes them suitable to be used with the conventional high-dose-rate (HDR) remote afterloading systems for interstitial brachytherapy. A recent in-water calibration experiment showed that the measured gamma dose rates near the new source are slightly greater than the neutron dose rates; contradicting the well established neutron-to-gamma dose ratio of approximately 2:1 at locations near a ^{252}Cf brachytherapy source. Specifically, the MCNP-predicted gamma dose rate is a factor of two higher than the measured gamma dose rate at the distance of 1 cm, and the differences between the two results gradually diminish at distances farther away from the source. To resolve this discrepancy, we updated the source gamma spectrum by including in the ORIGEN-S data library the experimentally measured ^{252}Cf prompt gamma spectrum as well as the true ^{252}Cf spontaneous fission yield data to explicitly model delayed gamma emissions from fission products. We also investigated the bremsstrahlung x-rays produced by the beta particles emitted from fission-product decays. The results show that the discrepancy of gamma dose rates is mainly caused by the omission of the bremsstrahlung x-rays in the MCNP runs. By including the bremsstrahlung x-rays, the MCNP results show that the gamma dose rates near a new ^{252}Cf source agree well with the measured results and that the gamma dose rates are indeed greater than the neutron dose rates.

The calibration experiment also showed discrepancies between the experimental and computational neutron dose profiles obtained. Specifically the MCNP-predicted neutron dose rates were ~25% higher than the measured neutron dose rates at all distances. In attempting to

resolve this discrepancy the neutron emission rate was verified by the National Institute of Standards and Technology (NIST) and an experiment was performed to explore the effects of bias voltage on ion chamber charge collection. So far the discrepancies between the computational and experimental neutron dose profiles have not been resolved. Further study is needed to completely resolve this issue and some suggestions on how to move forward are given.

CHAPTER 1

INTRODUCTION

The neutron has long been considered as a possible weapon in the fight against cancers that are resistant to conventional X-rays [1]. As early as the 1960's, researchers were considering the feasibility and effectiveness of methods using neutrons. However, during this time interest was mainly in using external beams of fast neutrons as a treatment method (EBFNT) [2]. Consequently, research in neutron brachytherapy (NBT) using neutron-emitting isotope, ^{252}Cf, was limited. Studies based on EBFNT would go on to show that significant late effect due to damage to healthy tissue would be an issue especially for deep-seated tumors. Because of this neutron therapy so far has only limited use in cancer treatment, most notably for salivary cancer [3]. The limited NBT studies, mainly conducted by Dr. Maruyama during the 1980's [4], on the other hand, have shown some positive results. Because NBT delivers more focused dose distribution in and around the tumor volume than does EBFNT, it is reasonable to believe that the late effect that plagued EBFNT may not be much of an issue for NBT.

While Dr. Maruyama did have success with his clinical trials on NBT, his study during the 1980's was limited due to the large size of the ^{252}Cf sources that were available to him [5]. Using the so-called AT sources he was forced to focus on intracavitary treatment of cervical cancers. In 2002 the Oak Ridge National Laboratory (ONRL) in conjunction with the Isotron Inc. developed a smaller and yet more intense medical grade source which would allow NBT to be used to treat cancers in other areas of the body [6]. An additional advantage of the smaller Isoton source is that it can be handled using remote after-loading systems currently in use today

by methods such as ^{192}Ir interstitial therapy. When compared to the manual afterloading techniques used by Dr. Maruyama, remote afterloading leads to more accurate source placement, and more predictable dose profiles around the source and tumor. Another important benefit is that a remote afterloading system is much safer for the medical personnel to handle ^{252}Cf sources.

However, before the new Isotron sources can be used clinically, they must first be properly calibrated and characterized. While ^{252}Cf emits neutron, beta, alpha, and gamma radiation as well as fission products, only neutrons and gamma photons penetrate the source capsule and contribute to radiation dose in the materials external to the source. The dose calibration experiments, including measurements of neutron and gamma dose profiles in water near an Isotron source, were recently performed at the Georgia Institute of Technology. However, discrepancies were found between the measured dose profiles and the dose profiles obtained computationally [7]. Specifically, the measured neutron absorbed dose rates were approximately 25% lower than that predicted by the Monte Carlo code, MCNP [8]. The measured gamma absorbed dose rates near the source, on the other hand, are significantly higher (by a factor of 2) than that predicted by MCNP. The current study is an attempt to resolve these discrepancies.

Chapter 2 provides detailed descriptions of the Isotron source. Chapter 3 describes the various possibilities that might have caused the discrepancies in detail. Chapter 4 discusses the methods used to resolve the discrepancies. The results are presented in Chapter 5. Chapter 6 provides conclusions from the current study and offers possible explanations for the remaining issues.

CHAPTER 2

DECAY PROPERTIES OF CF-252 AND DESCRIPTION OF ISOTRON SOURCE

Californium-252 has a half-life of 2.65years, and it decays via either alpha emission (96.9%) or spontaneous fission (3.1%). An average of 3.7 neutrons are emitted in each spontaneous fission. Approximately $2.31x10^6$ neutrons sec^{-1} µg^{-1} are emitted as a result of this decay [9]. The relatively high neutron yield and long half-life, when compared to other spontaneous fissioning isotopes, make ^{252}Cf the best isotope choice for developing a source for NBT. Cf-252's spontaneous fission neutron spectrum is similar to a fission reactor's in shape with an average energy of 2.1 MeV and a most probable energy of 0.7 MeV [9].

The first fabrications of medical Cf-252 sources were developed at Savannah River National Lab and involved one or more encapsulated Pd-Cf$_2$-O$_3$ cermet wires placed inside of an applicator tube [2] . These sources will be referred to hereafter as AT sources. The AT sources were used by Dr. Maruyama et al in clinical trials at the University of Kentucky [4]. Each AT source was approximately 2.8mm in diameter, 23mm long, had an active length of 15 mm, and contained between 10-30 µg of ^{252}Cf. At this size the sources could only be used for intracavitary treatments. Fabrication of smaller sources using these older techniques was possible, however, the sources produced contain less than 1µg of ^{252}Cf which is too small a quantity to be practically used for NBT. In order for NBT to move forward it was deemed necessary to develop smaller and yet more intense ^{252}Cf sources that could be used not only for intracavitary treatments but for interstitial treatments as well.

In 2002, under a Cooperative Research and Development Agreement (CRADA) with Isotron, Inc.(a start-up company located in Alpharetta, Georgia), the ORNL successfully

encapsulated a new generation of medical grade ^{252}Cf sources. These Isotron sources are much smaller and yet more intense than the AT sources used in the pervious studies, and as a result they have made NBT practical in both intracavitary and interstitial treatments. Each Isotron source contains approximately 90μg of ^{252}Cf in the form of a Pd-Cf$_2$-O$_3$ cermet wire. This is more than three times the amount found in the AT sources. The larger quantities of ^{252}Cf in the Isotron sources necessarily result in higher dose rates, which in turn, lead to reductions in treatment time. Figure 2.1 shows the geometric configuration of the Isotron source. The Isotron source has an outside diameter of 1.1mm, and its total length is approximately 8mm with an active length of 5mm. The ^{252}Cf cermet wire is encapsulated around a 0.2mm thick Pt-10%Ir wall. As a comparison, the AT source uses a Pt-10%Ir wall/ Pt-Ir sheath double encapsulation system with a total thickness of 0.7mm. The rule of thumb for the AT sources has been that the neutron-to gamma dose ratio in water (or tissue) is approximately 2:1 [10]. Because the mean free path of fission neutrons is much greater than a few mm, the thinner capsule wall (by 0.5 mm) of the Isotron source should not affect the neutron dose rate. However, the thinner capsule wall would allow some low energy photons to escape the source. As such, one should expect higher gamma dose rates in water (or tissue) within short distances from the source.
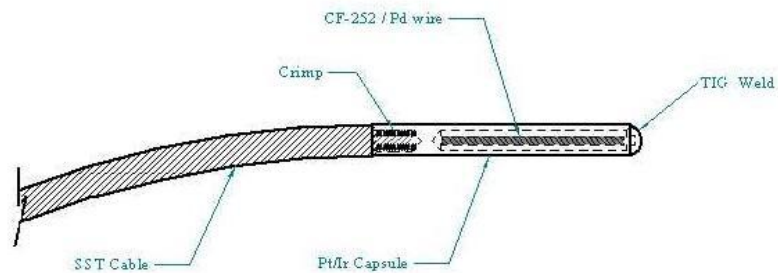
Figure 2.1 Geometric configuration of the Isotron source.

CHAPTER 3

DISPREPANCIES FROM THE PREVIOUS DOSE CALIBRATION STUDY

In October 2007 a study was conducted at the Georgia Institute of Technology to obtain both neutron and gamma dose profiles in water surrounding an Isotron ^{252}Cf source [7]. These profiles were obtained using both computational and experimental methods.

The experimental method was based on the use of two ion chambers i.e. the dual ion-chamber method. This method has long been used and accepted when trying to obtain dose in a mixed neutron/gamma field. The method involves taking measurements of the field using one ion chamber which is sensitive solely to gamma radiation and then taking another measurement using an ion chamber which is sensitive to both gamma and neutron radiations. In the case of the 2007 study, two ion chambers with model names M1 and T1, manufactured by Standard Imaging Inc., were used. These two chambers are alike in every way except for chamber wall material. Using these two detectors ensures that any differences in charge collection are due solely to gamma or neutron sensitivity and not an inherent manufacturing difference between the chambers. M1 which has a magnesium wall is predominantly sensitive to gamma rays. T1 has a chamber wall composed of A-150 tissue equivalent plastic, and is sensitive to both neutron and gamma radiation.

The measurements were taken with the Isotron source placed at the center of a water phantom 20 cm in both height and diameter. The ion chambers were placed at various distances from the source. The electric charge (Q) collected by an ion chamber at each position is directly

related to the neutron dose (D_n) and gamma dose (D_γ) at that position by Equation 3.1 below [11].

$$Q_{n,\gamma} = AD_\gamma + BD_n \qquad\qquad \text{(Eq. 3.1)}$$

where coefficients A and B are the ion chamber's response per unit absorbed dose due to gamma rays and neutrons respectively. Because A and B are known for the two chambers, the two measured Q values (from the two chambers) can then be used with Eq. (3.1) to obtain the corresponding neutron and gamma doses D_n and D_γ.

The computational method was based on the use of the Monte Carlo N-Particle code, MCNP5 [8], which is widely used and accepted in carrying out neutron and gamma ray transport calculations. In each calculation, the MCNP code follows the random walk of one source particle at a time for a large number of particle histories and the absorbed doses are obtained by tallying the energy depositions at various positions in the water phantom. It is known that the absorbed dose in water surrounding a sealed ^{252}Cf source is mainly contributed from three radiation components, the spontaneous fission neutrons, the primary gamma photons directly emitted from spontaneous fissions and fission product decays, and the secondary 2.2 MeV gamma photons that arise from the ^{1}H (n_{th}, γ)^{2}H reactions in water. As such it was easiest to consider each of these components separately and combine the results accordingly. Each MCNP run was made assuming that the Isotron source was at the center of a water phantom with 20 cm height and 20 cm diameter. Ring tallies that record energy depositions were placed at various distances from the source throughout the phantom.

To calculate the neutron dose profile, the neutrons emitted from the ^{252}Cf source were assumed to follow a Maxwellian energy distribution.

$$N(E) = Ce^{-\frac{E}{1.42}}E^{0.5}$$
(Eq. 3.2)

These neutrons were assumed to emit isotropically from the source and the absorbed dose rates were estimated assuming charged particle equilibrium (CPE). This assumption was possible due to the fact that the charged particles produced via neutron interactions have ranges shorter than the dimensions of the ring tallies (.2 mm radial& axial). By assuming CPE, a F6 tally providing an estimate of KERMA, could be used by MCNP. Under CPE, KERMA is equal to absorbed dose[11]. As such, the neutron dose profile could easily be obtained.

The gamma dose profile was obtained using a slightly different method. First, the primary gamma rays directly emitted from the spontaneous fissions and fission-product decays were considered. A spectrum obtained from ORNL was used in MCNP as an approximation to the magnitude and energy distribution of the photons emitted as a result of these two processes. A separate MCNP run was made to account for the secondary gamma photons arising from the ^{1}H (n_{th}, γ) ^{2}H reactions in water. In this case the energy of neutrons was again assumed to follow the Maxwellian distribution of Eq. (3.2) and the neutrons were emitted isotropically. For both the primary and secondary gamma dose calculations, MCNP used a more time-consuming tally, *F8, instead of the KERMA tally F6. This is due to the fact that photons interacting in water will lead to the production of electrons which have a range larger than the tally dimensions and as such CPE does not exist. Tally *F8 is more time-consuming because MCNP must follow the electrons produced by the photons to obtain the amount of energy deposited (by the electrons) in each tally. Despite the increase in computer time, we were still able to run 50000000 particle histories for both the primary and secondary calculations. The results of the primary calculation along the transverse axis had an uncertainty of less than 1% while the secondary calculation

7

had uncertainties <4% at distances far from the source. Near the source which is were we focused the uncertainties were again less than 1%. The energy deposition given by MCNP can then be converted to the absorbed dose for each tally.

Figure 3.1 shows the neutron dose profile obtained in the previous study both experimentally and by using MCNP [7]. As shown, the MCNP-obtained dose rates at various distances from the source are consistently higher than the dose rates obtained experimentally. The difference is approximately 25%.
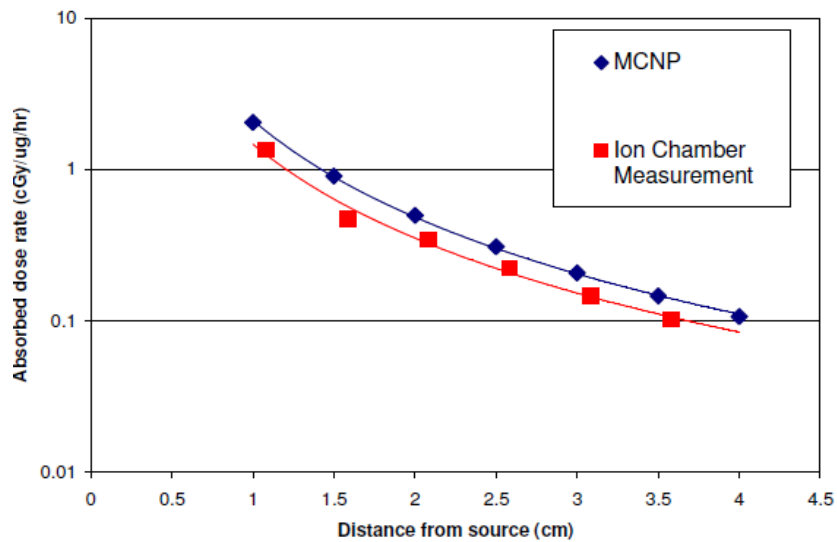
Figure 3.1. Neutron dose profile (along transverse axis) obtained in the previous study [7].

The MCNP-obtained primary and secondary gamma dose profiles were combined into one, which is shown in Fig. 3.2 along with the gamma dose profile obtained from the dual-ion chamber experiment [7]. Again discrepancies were found. The gamma dose rates at various distances from the source obtained experimentally were found to be consistently greater than

that obtained by MCNP. The differences between the two results are the greatest (~ a factor of two) at the distance of 1 cm, and fall to approximately 30% at distances 2 cm and beyond.
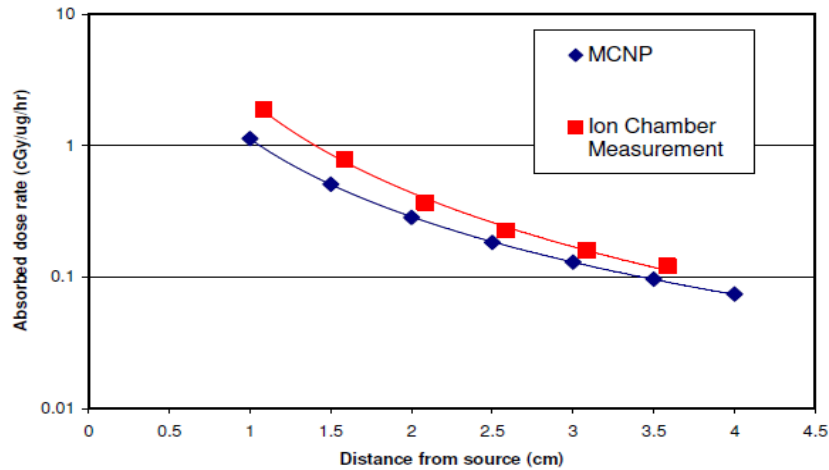
Figure 3.2. Gamma dose profile (along transverse axis) obtained in the previous study [7].

By comparing the measured results shown in Figs. 3.1 and 3.2, it was noticed that at distances close to ^{252}Cf source (<1.5 cm), the gamma dose was slightly greater than the neutron dose. This finding contradicts the well established rule of thumb that the neutron-to-gamma dose ratio near a ^{252}Cf source is 2:1. The finding implies that this rule of thumb will no longer apply when considering these new medical grade ^{252}Cf sources used for NBT. The focus of this current study was therefore to attempt to resolve the neutron and gamma dose profile discrepancies described above and to verify that the neutron-to-gamma dose ratio of 2:1 no longer applies when considering these new sources.

CHAPTER 4

METHODS FOR RESOLVING THE DOSE DISCREPANCIES

4.1 Methods for Resolving Neutron Dose Discrepancy

In the previous study, attempts were made to resolve the discrepancies found between the computational (i.e. MCNP) and the measured results [7]. As stated in Chapter 3, the neutrons emitted by the source were assumed to follow a Maxwellian energy distribution. After the discrepancy was found, the MCNP was run again with the neutrons behaving according to a Watt energy spectrum. This change, however, actually slightly increased the discrepancy between the two results.

Before any further changes were considered to the computational model or experimental method for this current study, the Isotron source was sent to The National Institute of Standards and Technology (NIST) to verify that the neutron emission rate provided with the source by ORNL was indeed accurate. Because the size of the Isotron ^{252}Cf source is so small when compared to most of the ^{252}Cf sources manufactured by ORNL, it was decided to verify the accuracy of its emission rate. NIST used the Manganese Sulfate Bath method to determine the neutron emission rate of the source. In this method the source is placed inside of a sphere of Manganese Sulfate. Then using a detector such as a scintillator detector one is able to count the number of photons emitted as a result of the ^{55}Mn (n,γ) reaction. After correcting this count rate to account for other n-reactions within the solution one is able to determine the number of neutrons emitted by any radioactive source. Using this method NIST found that the neutron emission rate provided by ORNL was indeed correct to within 1% [12]. With this being the

case, this study focused on possible adjustments that could be made to either the experimental method or computational model.

We first corrected a few errors made in the MCNP input files. The errors include the incorrect densities of the ^{252}Cf source and the Pt-Ir capsule wall. These changes, however, made a negligible difference in the computational results. We then considered the experimental factors. Because the dual-ion chamber method is such a widely accepted method for obtaining the absorbed doses of neutrons and gamma rays within a mixed n+γ field, any further experimentation would continue to be based on this method. After some research of other similar experiments using this method, it was discovered that, in most cases, a bias voltage of at least 500 V was used when taking measurements with the ion chambers in the mixed n+γ field [10]. The previous study used a bias voltage of 300 V [7], leading to possible incomplete charge collection when taking the measurements. To explore this possibility, an experiment was performed using the both the Standard Imaging electrometer, Max-4000, (which was used in the previous study and has a bias voltage of up to 300 V) and the Keithley Model 6517A Electrometer.

In this experiment the T1 chamber was connected to the Max-4000 electrometer. It was then used to take a measurement at 1.085 cm from the ^{252}Cf source which was placed at the center of an empty phantom. This measurement was made to establish the baseline result for the 300 V bias voltage. The T1 chamber was then connected to the Keithley Model 6517A and measurements were taken with bias voltages of 300V, 500V, 800V, and 1000V, which is the maximum recommended voltage for the T1 ion chamber. If there was indeed incomplete charge

collection, this experiment will determine exactly how much of an underestimation the results of the previous study were and a correction to those results can then be made accordingly.

4.2 Methods for Resolving Gamma Dose Discrepancy

Because the gamma dose discrepancy was most pronounced at distances less than 1.5 cm from the ^{252}Cf source, it was believed that the number of low energy photons emitted from the source was underestimated. This is based on the fact that photons with energies below 20 keV tend to deposit their energy in the first 1 cm when traveling in water so underestimating the contribution of these photons would greatly decrease the dose near the ^{252}Cf source. Two aspects of the previous study were therefore reviewed. First, the ^{252}Cf gamma spectrum used in the MCNP runs was reviewed, and any corrections that would lead to a more accurate spectrum (especially in the energy range below 20 keV) were made. Second, the effects of bremsstrahlung radiation were considered. Up until now when dealing with ^{252}Cf sources the effects of bremsstrahlung were generally considered negligible.

The gamma spectrum used in the MCNP input file in the previous study was supplied by Martin at ORNL [9]. Martin used ORIGEN-S, a module of ORNL's SCALE package [13] to obtain his spectrum. ORIGEN-S is a program that calculates the time-dependent concentrations of numerous nuclides in a given system such as a reactor core. For example given the concentrations of nuclides inside of a nuclear reactor core at some time t, ORIGEN-S is able to determine the nuclide composition(or inventory) of the core at any time after t. Decays, fissions, capture reactions, and leakage from the reactor core all lead to changes in nuclide concentrations within the reactor core. All of these changes as well as others are taken into consideration by ORGIEN-S. ORIGEN-S is a very powerful tool for keeping track of and

calculating how isotopes and systems change over time. However, ORIGEN-S was designed to consider systems such as reactor cores which undergo neutron-induced fission. Its ability to handle systems based around a spontaneously fissioning isotope was unknown and needed to be explored before the reliability of the gamma spectrum could be verified. In conjunction with Dr. Ian C. Gauld at ORNL, the methodology used by ORIGEN-S to handle the spontaneous fission of ^{252}Cf was reviewed and improved during this study. These improvements allow a more accurate gamma spectrum to be obtained which, in turn, improves the accuracy of the gamma dose profile obtained from MCNP runs.

Like neutron-induced fissions, spontaneous fissions lead to the buildup of a large number of fission products. In the case of neutron-induced fission, ORIGEN-S is able to keep track of the buildup and decay of each of these fission products. Because these fission products undergo beta and gamma decays, which may significantly contribute to the gamma doses in water surrounding the ^{252}Cf source, it is necessary to know how prevalent they are within a given system. Prior to this study, however, ORIGEN-S did not have the capability to keep track of fission product build-up during spontaneous fission. The concentration of the fissioning isotope (i.e. ^{252}Cf) was reduced correctly with respect to time, but the only build-up concentrations that were correctly calculated were those associated with other decay modes (i.e. alpha decay). Because gamma rays emitted from a sealed ^{252}Cf source are attributed to both the spontaneous fissions and the fission product decays, gamma ray intensity (or spectrum) can vary greatly as the fission products build up over time. To obtain an accurate gamma spectrum, it is therefore necessary to know the fission product concentrations. Previously, in an effort to deal with this issue the developers of ORIGEN-S used a series of approximations to account for gammas emitted by both the spontaneous fissions and the fission products.

According to the ORIGEN photon library manual [14], it is first assumed that the prompt gamma spectrum for ^{252}Cf spontaneous fissions is identical to the spectrum for neutron-induced fissions of ^{235}U. It is then proposed that the equilibrium spectrum of gamma rays emitted from fission-product decays (i.e. the delayed gamma spectrum) also has the same spectrum, but its intensity is approximately 0.75 of that for neutron-induced fissions of ^{235}U. These two approximations combine to become Equation 4.1 below, which was the spectrum used in ORIGEN-S. [14]

$$N(E) = 11.5 \qquad\qquad\qquad 0.1 \leq E \leq 0.6 \text{ MeV} \qquad \text{(Eq. 4.1a)}$$

$$N(E) = 35.4e^{-1.78E} \qquad\qquad 0.6 \leq E \leq 1.5 \text{ MeV} \qquad \text{(Eq. 4.1b)}$$

$$N(E) = 12.6e^{-1.09E} \qquad\qquad 1.5 \leq E \leq 10.5 \text{ MeV} \qquad \text{(Eq. 4.1c)}$$

$$N(E) = 0 \qquad\qquad\qquad E < 0.1 \text{ or } E > 10.5 \text{ MeV} \qquad \text{(Eq. 4.1d)}$$

where $N(E)$ = number of photons at energy E, in, photons fission^{-1} Mev^{-1} and E is in MeV.

Because ORIGEN-S is generally used for shielding calculations when dealing with spontaneous fission, this approximate spectrum was adequate for what the developers were trying to do. In this study, however, a highly accurate ^{252}Cf gamma spectrum is required because the desire is to obtain a gamma dose profile near the source with the highest quality.

In order to improve the accuracy of the gamma spectrum associated with ^{252}Cf and other spontaneous fissioning isotopes, the capability to keep track of spontaneous fission product concentrations was added into ORIGEN-S. This was done by incorporating into the ORIGEN decay library the fission product yield data of ^{252}Cf as well as six other isotopes that undergo spontaneous fission. These data were taken from ENDF/B-VII. A FORTRAN-based computer program was written to incorporate the fission product yields into the library in a manner

similar to that already used by ORIGEN-S. The ORIGEN-S transition matrix was then rebuilt

to include these new data. The transition matrix is what ORIGEN-S uses to solve a coupled set

of differential equations. These equations give way to the time-dependent nuclide

concentrations of each nuclide found in the ORIGEN library. Once the nuclide concentrations

are known, ORIGEN-S can simply use the existing data in the photon library to calculate the

photon spectrum associated with the decay of the fission-product nuclides. This spectrum

represents the true energy distribution for the time-dependent photon intensity rather than the

approximation used in the previous study.

Once ORIGEN-S was able to calculate the accurate fission-product gamma spectrum, it

was no longer necessary to use the spectrum given by Equation 4.1 above. Since Equation 4.1

accounts for both the prompt and delayed gamma rays, simply using Equation 4.1 in addition to

our results would lead to double counting of the delayed gammas. This could be avoided by

dividing Equation 4.1 by 1.75 to remove the 0.75 factor. However, it has been shown by

Verbinski et al [15] that the prompt gamma spectrum of fissioning isotopes does change with Z

number (See Figure 4.1). Between 700 keV and ~ 6 MeV the three spectra are basically the

same but as the mass number of the fissioning nuclide increases the amplitude of the spectrum

below 700 keV increases. Because the low energy photons might contribute greatly to the

gamma dose near the source (which therefore may resolve the gamma dose discrepancy), it was

therefore decided to replace the prompt gamma spectrum with a more accurate, up-to-date

spectrum.

The prompt gamma spectrum incorporated into ORIGEN-S is the [252]Cf spectrum shown

in Fig. 4.1 obtained by Verbinski et al. Due to the constraints of Verbinski's experiment this

spectrum only contains gamma rays with energies above 140 keV. In order to get the spectrum

into a format that could be used by ORIGEN-S, the Verbinski spectrum was digitized using
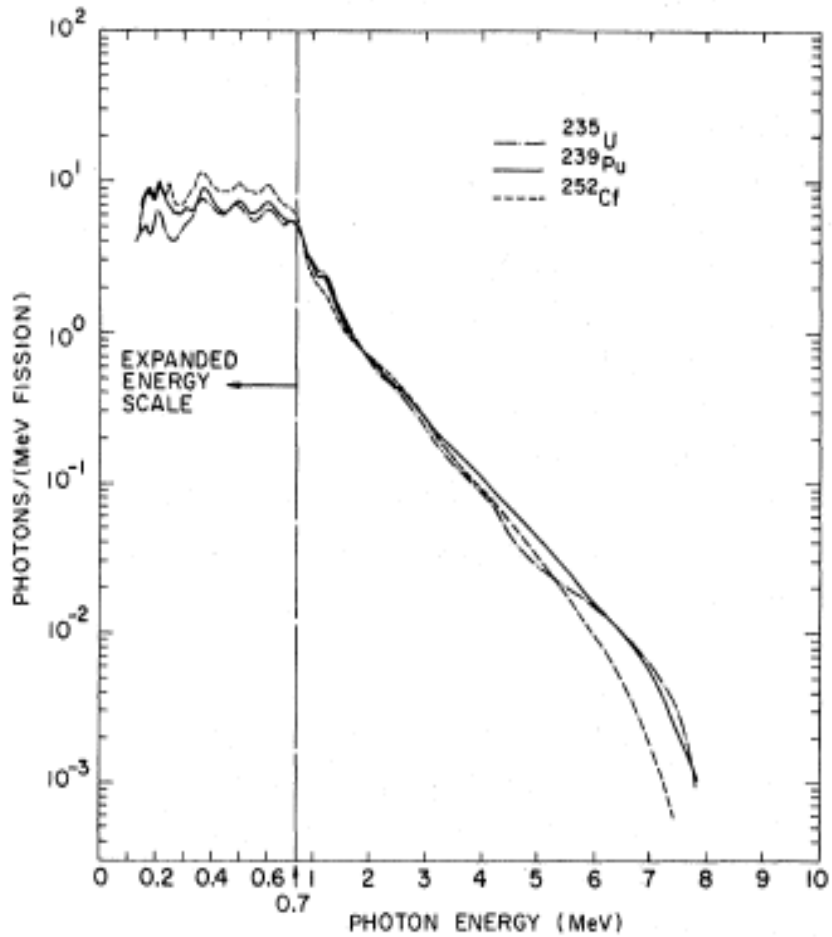
DigXY[16].

Figure 4.1. The measured unfolded prompt gamma spectrum for ^{235}U, ^{239}Pu, and ^{252}Cf [15].

This spectrum was placed into the ORIGEN-S library, and a time-dependent total (i.e.

prompt + delayed) gamma spectrum was then obtained using the new data library. This

spectrum along with the spectrum used in the previous study [7] are shown in Table 4.1.

Table 4.1. ^{252}Cf gamma spectrum in the previous Study [7] vs. current study

Energy (MeV)	Photons sec^{-1}µg^{-1}	Energy (MeV)	Photons sec^{-1}µg^{-1}
0.01-0.10	7.32E+05	0.0100-0.0115	6.87E+03
0.10-0.20	2.52E+03	0.0115-0.0133	1.30E+02
0.20-0.30	3.54E+06	0.0133-0.0153	1.19E+06
0.30-0.40	7.59E+03	0.0153-0.0177	1.20E+04
0.40-0.60	5.24E-01	0.0177-0.0204	1.62E+05
0.60-0.80	3.07E+06	0.0204-0.0235	6.12E+04
0.80-1.00	5.63E-02	0.0235-0.0270	1.55E+04
1.00-1.33	1.26E+06	0.0270-0.0312	5.42E+04
1.33-1.66	0.00E+00	0.0312-0.0359	8.53E+04
1.66-2.00	5.51E+05	0.0359-0.0429	1.27E+05
2.00-2.50	3.34E+05	0.0429-0.0495	2.04E+04
2.50-3.00	1.94E+05	0.0495-0.0571	1.65E+04
3.00-4.00	1.74E+05	0.0571-0.0658	3.66E+04
4.00-5.00	5.88E+04	0.0658-0.0758	4.05E+04
5.00-6.50	2.36E+04	0.0758-0.0874	3.29E+04
6.50-8.00	4.63E+03	0.0874-0.101	4.06E+04
8.00-10.00	9.83E+02	0.101-0.116	9.17E+04
Total	9.96E+06	0.116-0.134	6.00E+04
		0.134-0.154	3.53E+05
		0.154-0.178	8.57E+04
		0.178-0.205	1.04E+05
		0.205-0.236	1.25E+05
		0.236-0.273	6.92E+05
		0.273-0.314	2.25E+05
		0.314-0.362	8.13E+05
		0.362-0.417	1.95E+05
		0.417-0.481	7.69E+05
		0.481-0.555	8.61E+05
		0.555-0.85	1.57E+06
		0.85-1.30	1.17E+06
		1.30-1.99	8.60E+05
		1.99-3.05	5.92E+05
		3.05-5.39	1.85E+05
		5.39-9.79	1.03E+04
		Total	1.07E+07

As shown, the resolution of the spectrum obtained using the new ORIGEN-S library is much better than the one used in the previous study. While the total intensity of the new spectrum is only 7% higher than that of the old spectrum, the intensity for photons with energies below 100 keV (of the new spectrum) is more than a factor of two higher. The low-energy photons, if they escape the source capsule, tend to deposit their energies at distances near the source, the abundant low-energy photons (of the new spectrum) therefore could explain the previously observed increase in gamma dose rates nearby the new ^{252}Cf source. To

18

more closely examine the dose contribution due to the low energy photons, an MCNP run was made using a surface tally F1 immediately surrounding the source capsule to obtain the spectrum of gamma photons leaking out of the source capsule (the leakage gamma spectrum). Figure 4.2 shows the source capsule geometry and the F1 tally modeled in the MCNP runs.
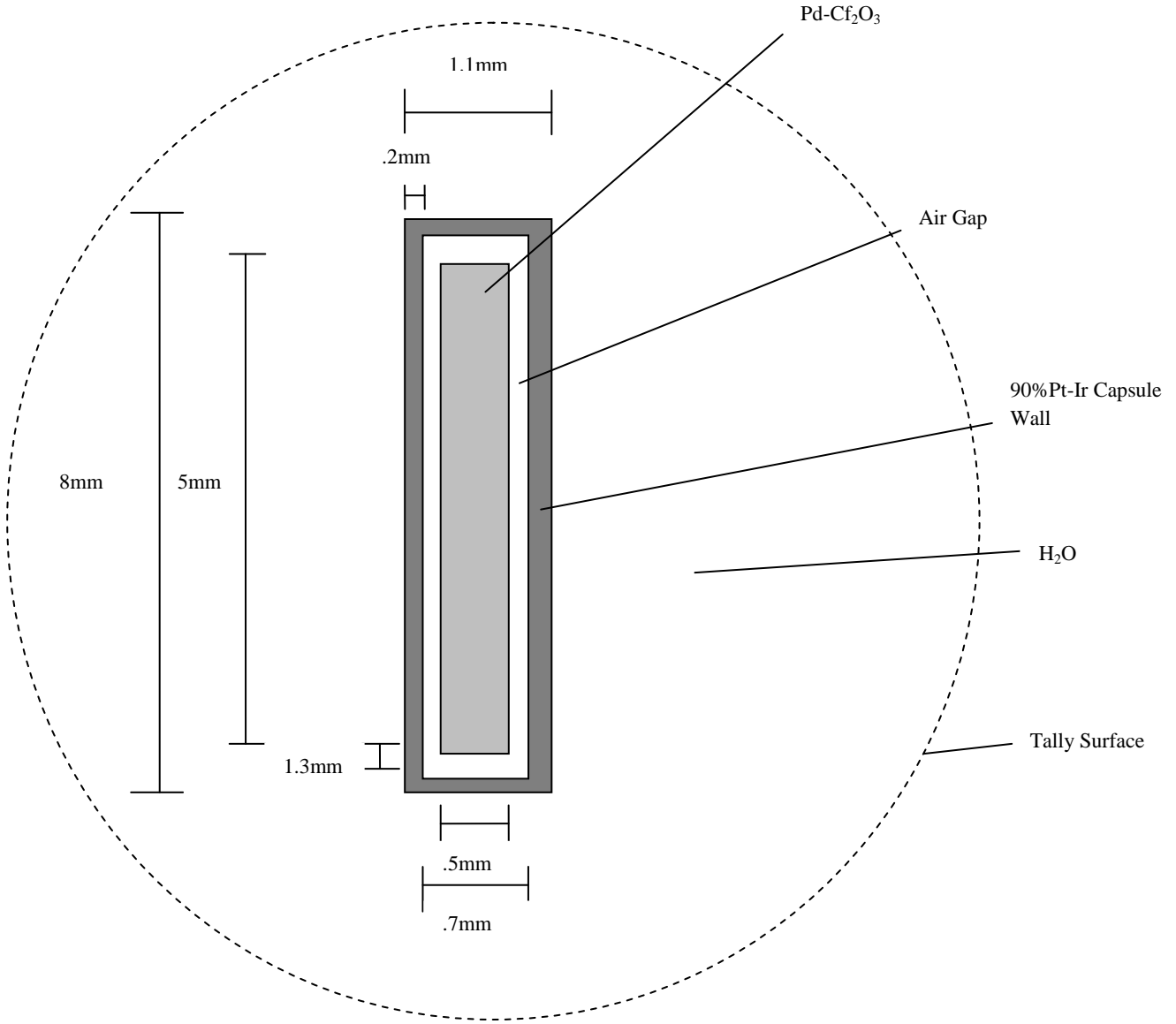

Figure 4.2 The source capsule geometry and the F1 tally modeled in the MCNP run to obtain the leakage gamma spectrum.

Until now it was assumed that the only particles that significantly contributed to dose near a ^{252}Cf source were neutrons and photons. This assumption was indeed valid when dealing with larger sources such as the AT sources used by Maryuma et al. However, as described below, this assumption is not valid when dealing with the new Isotron sources having a much thinner capsule wall. The fission products produced by ^{252}Cf spontaneous fissions generally undergo beta decay. These beta particles are able to contribute to the dose outside the source either by escaping the capsule wall or more likely by interacting within the source wall leading to the production of bremsstrahlung X-rays, which in turn, escape the capsule wall. Neither of these effects was accounted for in the previous study. Not accounting for the beta particles or bremsstrahlung x-rays escaping the source could be another factor why the dose rates were much higher for the measured gamma dose profile. The difference between the measured and the MCNP results was most pronounced near the source, which is exactly where these particles would deposit their energies. To explore the bremsstrahlung X-ray contribution to the gamma dose profile, a program called BETA-S [17] was used. BETA-S was developed by Dr. Ian C. Gauld and is used in conjunction with ORIGEN-S. BETA-S tracks the intensity and energy of beta particles emitted by decaying fission products. Using this program it was shown that over 3.8×10^6 betas sec^{-1} μg^{-1} are emitted within the source. The beta energy spectrum shown in Fig. 4.3 was obtained and input into MCNP to calculate the effect on gamma dose profile near the source in the water phantom. For this run 30000000 particle histories were run and uncertainties along the transverse axis were .5-1.5% at distances < 2cm from the source. Because the range of the beta particles emitted is extremely small, one would expect that the largest contribution to the dose comes from the bremsstrahlung X-rays escaping the capsule wall. As such, an additional MCNP run was also made with the geometry similar to that

described in Fig. 4.2 to obtain the spectrum of bremsstrahlung X-rays escaping the capsule wall

(the leakage bremsstrahlung X-ray spectrum).
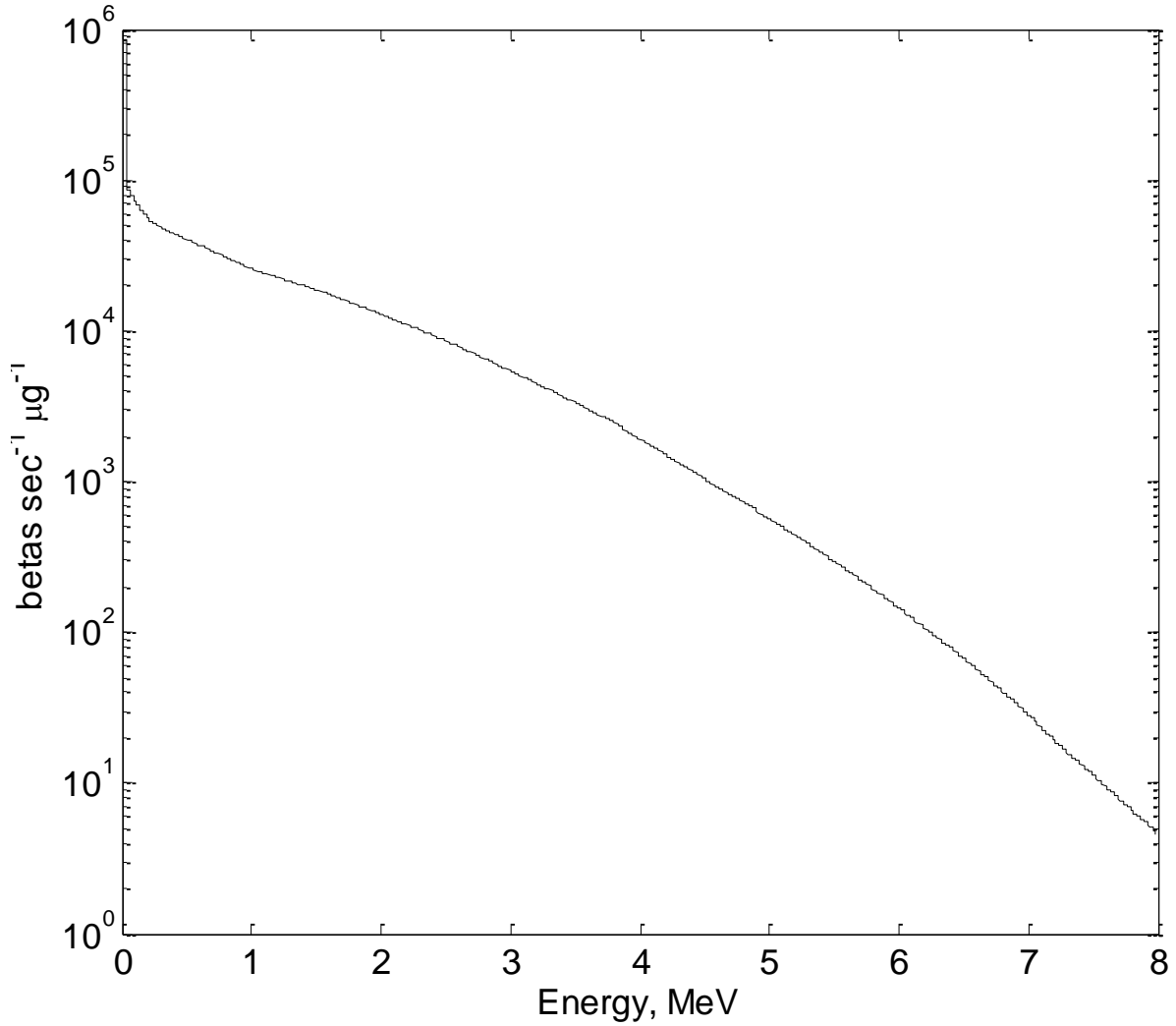
Figure 4.3. The beta spectrum of ^{252}Cf fission products obtained with BETA-S [17].

CHAPTER 5

RESULTS

5.1 Neutron Dose

The results from the experimental measurements are shown below. Measurements were taken with the T1 ion chamber being connected to either the Max-4000 electrometer or the Keithley Model 6517A electrometer. Counts were taken near the source until an equilibrium charge collection rate was achieved. As can be seen from Table 5.1, the amount of charge collected was unaffected by increasing the bias voltage from 300V to 1000V. From these results it can be concluded that incomplete charge collection was not a factor in causing the discrepancies in the previous study. Therefore, the discrepancy between the experimental and computational neutron dose profiles is still unresolved.

Table 5.1 Experiment to determine dependence of charge collection on bias voltage

Electrometer	Max-4000	Keithley Model 6517A			
Bias Voltage (V)	300	300	500	800	1000
Charge Collection (pA)	.209	.203	.207	.209	.209

5.2 Gamma Dose

5.2.1 Gamma dose due to the new source gamma spectrum

The gamma dose profile obtained with MCNP using the new source gamma spectrum (Table 4.1) is shown in Table 5.2 along with the dose profile previously obtained using

Equation 4.1. As shown, the new spectrum actually led to a decrease in dose of ~15% over the entire range of distances.

Table 5.2   The gamma dose profile obtained with MCNP using the old source gamma spectrum (i.e. previous study) vs. that using the new source gamma spectrum (i.e.this study).

Transverse Distance (cm)	Gamma Dose (cGy/µg-hr)	
	Previous study	This study
0.5	4.258	3.566
1.0	1.133	0.949
1.5	0.511	0.426
2.0	0.285	0.2419
2.5	0.184	0.1576
3.0	0.130	0.1111
3.5	0.097	0.0833
4.0	0.074	0.0644
4.5	0.060	0.0518
5.0	0.049	0.0427
5.5	0.041	0.0356
6.0	0.0362	0.0316

The decrease in gamma dose especially for distances less than 1.5 cm from the source was somewhat a surprise because Table 4.1 clearly shows that the intensity for photons with energies below 100 keV (of the new spectrum) is significantly higher than the old spectrum used in the previous study. This "surprise", however, can be explained by careful examination of "the leakage spectrum" (shown in Fig. 5.1), which is the spectrum of gamma rays that

actually escape the source capsule. As described in Chapter 4.2, the leakage spectrum was

obtained by MCNP using a spherical surface tally (F1 type) immediately surrounding the

source capsule. By comparing the two spectra shown in Fig. 5.1, it is clear that while the

source photons are abundant in the energy range between 13 and 15 keV, these photons are

fully attenuated by the source capsule and therefore do not contribute to the dose outside. The

strong attenuation of 15-keV photons by the capsule wall is also consistent with the fact that the

L-edge of Platinum and Iridium is ~14 keV and that these photons are easily absorbed by the

source capsule via the photoelectric effect. All together, the intensity of the leakage gamma

spectrum is actually lower than the old source gamma spectrum used in the previous study over

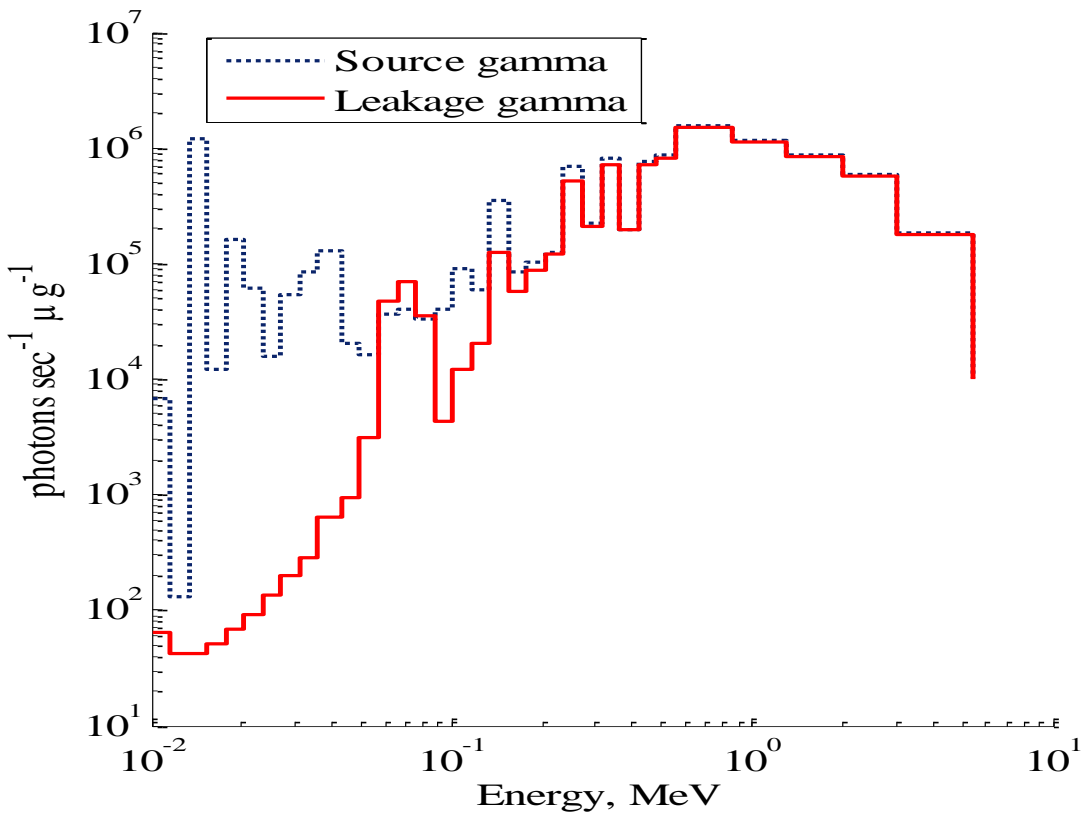the entire energy range, which lead to a slight decrease in gamma dose.

Figure 5.1 ^{252}Cf source gamma spectrum vs. leakage spectrum

In addition to the attenuation of gamma photons by the capsule wall, one must also consider the fact that the new prompt gamma spectrum that was placed into the ORIGEN library is much softer than the original spectrum found in the ORIGEN photon library. Using Equation 4.1 the ORIGEN library originally contained prompt gammas with energies up to 9.25 MeV. The new spectrum only has gamma energies up to ~7.5 MeV. This also leads to a slight decrease in dose at distances further from the source ($\geq$2cm).

5.2.2 Gamma dose due to the bremsstrahlung X-rays

Figure 5.2 shows the spectrum of bremsstrahlung x-rays escaping the source capsule versus the leakage gamma spectrum. As shown, the intensity of escaping bremsstrahlung x-ray photons is actually greater than the intensity of the leakage source gamma photons having energies below 60 keV. Consequently, omitting the bremsstrahlung x-rays will lead to a significant underestimation of dose near the source. Indeed, as shown in Table 5.3 the dose due to the bremsstrahlung X-rays is significantly higher than the dose due to source gamma rays for distances $\leq$ 2 cm. Also shown in Table 5.3 is the column of total "gamma dose", which was obtained by adding together the values of the first two columns of the Table. Obviously, the inclusion of the dose due to the bremsstrahlung x-rays greatly increases the total gamma dose at distances $\leq$ 2 cm. Figure 5.3 shows the two computationally obtained gamma dose profiles (with and w/o the bremsstrahlung X-ray contribution) as well as the measured gamma dose profile. As shown, by including the bremsstrahlung X-ray contribution the computationally obtained gamma dose profile now agrees quite well with the measured gamma dose profile.
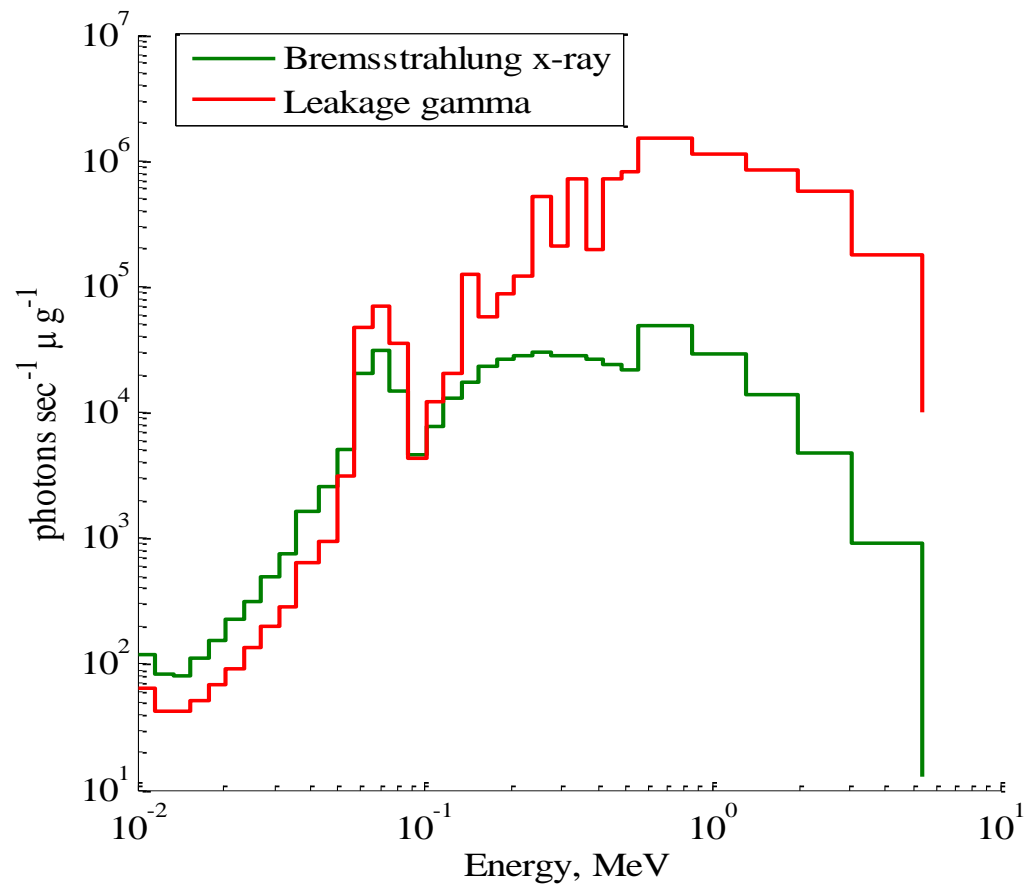
Figure 5.2 Leakage gamma spectrum vs. bremsstrahlung x-ray spectrum

Table 5.3 The bremsstrahlung dose profile versus the gamma dose profile.

Transverse Distance (cm)	Dose due to Bremsstrahlung X-rays (cGy/µg-hr)	Dose due to Source Gamma Rays (cGy/µg-hr)	Total "Gamma Dose" (cGy/ µg-hr)
0.5	9.242	3.566	12.808
1.0	1.2	0.949	2.149
1.5	0.191	0.426	0.617
2.0	0.035	0.2419	0.277
2.5	0.008	0.1576	0.1656
3.0	0.004	0.1111	0.1151
3.5	0.002	0.0833	0.0853
4.0	0.002	0.0644	0.0664
4.5	0.001	0.0518	0.053
5.0	0.001	0.0427	0.0437
5.5	0.001	0.0356	0.0366
6.0	0.001	0.0316	0.0326
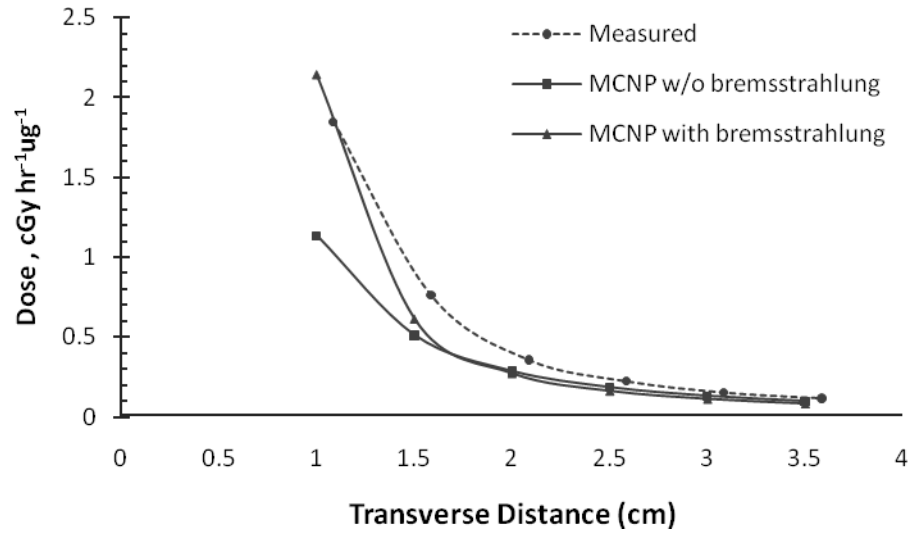
Figure 5.3 Computational vs. experimental gamma dose profiles.

5.3 Neutron-to-Gamma Dose Ratio

Now that the discrepancy between the computational and experimental gamma dose profiles has been resolved, it can be seen that the neutron-to-gamma dose ratio for the new medical grade ^{252}Cf sources does not follow the widely accepted rule of thumb of 2:1. In fact, one would expect that the dose ratio be a strong function of capsule wall thickness as well as the distance from the source. To illustrate such an effect, several MCNP runs were made for various capsule wall thicknesses. The results are shown in Table 5.4.

Table 5.4 Neutron-to-gamma dose ratio near the ^{252}Cf source

Capsule Thickness	Isotron						AT
	.1mm	.2mm	.3mm	.4mm	.5mm	.6mm	.7mm
Transverse Distance (cm)	Neutron-to-Gamma Dose Ratio						
0.25	0.299	0.543	0.886	1.287	1.647	1.958	2.174
0.5	0.349	0.601	0.933	1.301	1.635	1.911	2.106
1.0	0.636	0.942	1.279	1.595	1.838	2.008	2.124
1.5	1.160	1.449	1.693	1.874	2.000	2.094	2.148
2.0	1.637	1.819	1.901	1.983	2.043	2.087	2.123

Clearly, within the distance of 2 cm from the source, the neutron-to-gamma dose ratio increases with the distance and decreases with the source capsule thickness. This is due to the fact that the capsule wall is made of platinum and iridium and that even with a small fraction of a millimeter, these high-z materials still have high probabilities of absorbing low-energy bremsstrahlung x-rays and preventing them from contributing to the "gamma dose" outside the capsule. Table 5.4 also verifies the rule of thumb for the applicator tube (AT) sources since the ratio of the .7mm encapsulation was approximately 2 at all distances.

CHAPTER 6

CONCLUSIONS AND REMARKS

In this current study, discrepancies found previously between the computational and experimental ^{252}Cf gamma dose profiles were investigated and resolved. Modifications to the ORNL code ORIGEN-S were made as part of this investigation and subsequently ORIGEN-S can now be used to model systems based upon the spontaneous fission of seven isotopes. These isotopes in addition to ^{252}Cf include: ^{238}U, ^{244}Cm, ^{246}Cm, ^{248}Cm, ^{250}Cf, and ^{253}Es. The effects of bremsstrahlung X-rays emitted from the new Isotron ^{252}Cf source were also investigated and found to significantly affect the gamma dose profile. The bremsstrahlung X-rays, emitted as a result of fission products undergoing beta decays, was significant enough to account for the discrepancy observed previously between the computational and experimental dose profiles.

It has been shown that the effect of bremsstrahlung X-rays renders a widely accepted rule of thumb invalid when considering these new Isotron ^{252}Cf sources. The rule of thumb which states that the neutron-to-gamma dose ratio near a ^{252}Cf source is 2:1 was found to be untrue during this study. This is due to the fact that the new Isotron sources have a source capsule wall that is less than one-third the thickness of the AT sources used in previous studies. This thinner capsule wall allows more bremsstrahlung x-rays to escape the capsule wall and contribute to the dose outside. In fact, for distances less than 2 cm from the source, the neutron-to-gamma dose ratio is found to be strongly dependent on the source capsule wall thickness as well as the distance from the source.

The discrepancy between the computational and experimental ^{252}Cf neutron dose profiles was also investigated, but has not yet been resolved. The neutron emission rate was verified by NIST using the manganese sulfate bath method. The rate given by ORNL was found to be accurate. An experiment was performed to verify whether or not insufficient bias voltage had led to incomplete charge collection in the previous ion chamber measurements. The bias voltage was found to be sufficient ruling out the possibility of incomplete charge collection being the cause of the discrepancy. As a suggestion for future investigation, a possible reason for the neutron discrepancy may reside in the geometry of the ion chambers used for taking the experimental measurements. The actual collecting volume of the Standard Imaging thimble ion chambers has cylindrical sides and a half sphere at the tip. As a result, neutron and gamma interaction with the collecting volume is dependent upon which part of the collecting volume the particle is incident against. The response functions used in this experiment were based on purely spherical ion chambers, so it would be useful to conduct a study to see exactly how the geometry of this detector affects its response to both neutron and gamma rays.

Appendix A: ORIGEN/BETA-S Input Examples

Appendix A.1- ORIGEN-S Input

```
#origens
-1$$ 600000
0$$ a11 71 e t
Decay Case
3$$ 10 1 1 22 a16 0 a33 200 e t
35$$ 0 t
54$$ a1 7 a8 1 a11 0 e
56$$ a2 9 a6 1 a10 0 a13 6 a14 5 a15 3 a17 2 e
57** 0 a3 1e-05 e
95$$ 0 t
Case 1
0 MTU
60** 0 0.5 1 2 2.65 4 4.5 4.9945 7
61** f0.05
65$$
'Gram-Atoms  Grams  Curies  Watts-All  Watts-Gamma
 3z  1  0  0  3z  3z  3z  6z
 3z  1  0  0  3z  3z  3z  6z
 3z  1  0  0  3z  3z  3z  6z
81$$ 2 0 12 2 e
82$$ 2 2 2 2 2 2 2 2 2 e
83**
18i 1.0000000e+07 6.0000000e+06
179l 6.0000000e+06 1.0000000e+04
84**
 1.4920000e+07 1.2200000e+07 1.0000000e+07 8.1800000e+06
 6.3600000e+06 4.9600000e+06 4.0600000e+06 3.0100000e+06 2.4600000e+06
 2.3500000e+06 1.8300000e+06 1.1100000e+06 5.5000000e+05 1.1100000e+05
 3.3500000e+03 5.8300000e+02 1.0100000e+02 2.9000000e+01 1.0100000e+01
 3.0599990e+00 1.1200000e+00 4.1400000e-01 9.9999980e-03 e
73$$ 982520 982490 982500 982510 982530 982540
74** 3.54665e-07 7.70026e-09 3.74719e-08 1.1447e-08 4.11779e-12
 3.29423e-11
75$$ 2 2 2 2 2 2
t
56$$ 0 0 a10 1 e t
56$$ 0 0 a10 2 e t
56$$ 0 0 a10 3 e t
56$$ 0 0 a10 4 e t
56$$ 0 0 a10 5 e t
56$$ 0 0 a10 6 e t
56$$ 0 0 a10 7 e t
56$$ 0 0 a10 8 e t
56$$ 0 0 a10 9 e t
56$$ f0 t
end
```

Appendix A.2- BETA-S Input (Truncated)

```
#origens
-1$$ 600000
0$$ a11 71 e t
Decay Case
3$$ 10 1 1 22 a16 0 a33 200 e t
35$$ 0 t
54$$ a1 7 a8 1 a11 0  e
56$$ a2 9 a6 1 a10 0 a13 6 a14 5 a15 3 a17 2 e
57** 0 a3 1e-05 e
95$$ 0 t
Case 1
0 MTU
60** 0 0.5 1 2 2.65 4 4.5 4.9945 7
61** f0.05
65$$
'Gram-Atoms  Grams  Curies  Watts-All  Watts-Gamma
 3z   1   0   0   3z   3z   3z   6z
 3z   1   0   0   3z   3z   3z   6z
 3z   1   0   0   3z   3z   3z   6z
81$$ 2 0 12 2 e
82$$ 2 2 2 2 2 2 2 2 2 2 e
83**
18i 1.0000000e+07 6.0000000e+06
179l 6.0000000e+06 1.0000000e+04
84**
 1.4920000e+07 1.2200000e+07 1.0000000e+07 8.1800000e+06
 6.3600000e+06 4.9600000e+06 4.0600000e+06 3.0100000e+06 2.4600000e+06
 2.3500000e+06 1.8300000e+06 1.1100000e+06 5.5000000e+05 1.1100000e+05
 3.3500000e+03 5.8300000e+02 1.0100000e+02 2.9000000e+01 1.0100000e+01
 3.0599990e+00 1.1200000e+00 4.1400000e-01 9.9999980e-03 e
73$$ 982520 982490 982500 982510 982530 982540
74** 3.54665e-07 7.70026e-09 3.74719e-08 1.1447e-08 4.11779e-12
 3.29423e-11
75$$ 2 2 2 2 2 2
t
56$$ 0 0 a10  1 e t
56$$ 0 0 a10  2 e t
.
. condensed for space (Same as in App. A.1)
.
56$$ 0 0 a10  8 e t
56$$ 0 0 a10  9 e t
56$$ f0 t
end
=betas_linux64
10 65 71 6
Brem Spectrum
1 1 4 3 1
0.05 1
1
end
```

Appendix B- MCNP Input Examples

Appendix B.1- Neutron Dose Profile Example (Truncated)

```
Title
C CF-252 Secondary dose distribution in water phantom with default x-sec
C from Maxwellian fission spectrum
C   CELL CARDS
C source cell cards**********************************
2 0 1000  -2000     IMP:n=1 $ gap space
3 4 -21.53  2000 -3000 IMP:n=1 $ casing
4 3 -12  -1000  IMP:n=1 $ source
C 5  1 -1.0 3 -9999  IMP:n=1 $ water medium
9 0 9999          IMP:n=0 $ outside boundary
C top of source****************************************
100 2 -1 101 -102  1 -2 imp:n=1
101 2 -1 101 -102  2 -3 imp:n=1
102 2 -1 101 -102  3 -4 imp:n=1
103 2 -1 101 -102  4 -5 imp:n=1
104 2 -1 101 -102  5 -6 imp:n=1
105 2 -1 101 -102  6 -7 imp:n=1
106 2 -1 101 -102  7 -8 imp:n=1
107 2 -1 101 -102  8 -9 imp:n=1
108 2 -1 101 -102  9 -10 imp:n=1
109 2 -1 101 -102 10 -11 imp:n=1
110 2 -1 101 -102 11 -12 imp:n=1
111 2 -1 101 -102 12 -13 imp:n=1
112 2 -1 101 -102 13 -14 imp:n=1
113 2 -1 101 -102 14 -15 imp:n=1
114 2 -1 101 -102 15 -16 imp:n=1
115 2 -1 101 -102 16 -17 imp:n=1
116 2 -1 101 -102 17 -18 imp:n=1
117 2 -1 101 -102 18 -19 imp:n=1
118 2 -1 101 -102 19 -20 imp:n=1
.
. condensed for space
.
1350 2 -1 126 -127  1 -2 imp:n=1
1351 2 -1 126 -127  2 -3 imp:n=1
1352 2 -1 126 -127  3 -4 imp:n=1
1353 2 -1 126 -127  4 -5 imp:n=1
1354 2 -1 126 -127  5 -6 imp:n=1
1355 2 -1 126 -127  6 -7 imp:n=1
1356 2 -1 126 -127  7 -8 imp:n=1
1357 2 -1 126 -127  8 -9 imp:n=1
1358 2 -1 126 -127  9 -10 imp:n=1
1359 2 -1 126 -127 10 -11 imp:n=1
1360 2 -1 126 -127 11 -12 imp:n=1
1361 2 -1 126 -127 12 -13 imp:n=1
1362 2 -1 126 -127 13 -14 imp:n=1
1363 2 -1 126 -127 14 -15 imp:n=1
1364 2 -1 126 -127 15 -16 imp:n=1
1365 2 -1 126 -127 16 -17 imp:n=1
```

1366 2 -1 126 -127 17 -18 imp:n=1
1367 2 -1 126 -127 18 -19 imp:n=1
1368 2 -1 126 -127 19 -20 imp:n=1
C end of shells **
8 2 -1.0 -9999 127   imp:n=1
10 2 -1.0 -9999 -127 -1 101 imp:n=1
11 2 -1.0 20 -9999 -127 101 imp:n=1
12 2 -1.0 -101 3000 -9999   imp:n=1

C SURFACE CARDS
C Source terms
1000 RCC 0 0 -.25 0 0 .5 .025 $ source
2000 RCC 0 0 -.38 0 0 .76 .035 $ gap
3000 RCC 0 0 -.4 0 0 .8 .055 $ casing
9999 RCC 0 0 -10 0 0 20 10 $ outside boundary h=20cm and r=10cm
C planes **********************************
1 PZ -.05
2 PZ .05
3 PZ .4
4 PZ .6
5 PZ .9
6 PZ 1.1
7 PZ 1.4
8 PZ 1.6
9 PZ 1.9
10 PZ 2.1
11 PZ 2.3
12 PZ 2.7
13 PZ 2.8
14 PZ 3.2
15 PZ 3.3
16 PZ 3.7
17 PZ 3.8
18 PZ 4.2
19 PZ 4.3
20 PZ 4.7 $ end planes
C cylinders **************************
101 CZ .2825
102 CZ .3025
103 CZ .535
104 CZ .635
105 CZ .985
106 CZ 1.185
107 CZ 1.485
108 CZ 1.685
109 CZ 1.985
110 CZ 2.185
111 CZ 2.485
112 CZ 2.685
113 CZ 2.985
114 CZ 3.185
115 CZ 3.385
116 CZ 3.785
117 CZ 3.885
118 CZ 4.285

```
119 CZ 4.385
120 CZ 4.785
121 CZ 4.885
122 CZ 5.285
123 CZ 5.385
124 CZ 5.785
125 CZ 5.885
126 CZ 5.9
127 CZ 6.0    $ end shells

C  MATERIALS
m2  1001 2 8016  1 $ water medium
mt2 lwtr.60
C m3  46108 -2.5032 98252 -11.8556 8016 -1.1364 CF source assumed to be all Pd
m3 46102 .01001 46104 .1103 46105 .2211 46106 .2706 46108 .2619 46110 .1160&
96248 .002423 98252 .00091 8016 .006667
m4  77000 -10 78000 -90 $ Pt-10%Ir casing
SDEF ERG=D1 POS=0 0 0 CEL=4 RAD=D2 EXT=D3 AXS=0 0 1
SP1  -2  1.42 $ maxwellian fission spectrum
SI2 0 .024999
sp2 -21 0
SI3 -0.24999 0.24999
sp3 -21 0
*F6:N 100 101 102 103 104 105 106 107 108 109 110 111 &
112 113 114 115 116 117 118 150 151 152 153 154 155 156 &
157 158 159 160 161 162 163 164 165 166 167 168 ……
.
.  condensed for space
.
1300 1301 1302 1303 1304 1305 1306 1307 1308 1309 1310 &
1311 1312 1313 1314 1315 1316 1317 1318 1350 1351 1352 1353 &
1354 1355 1356 1357 1358 1359 1360 1361 1362 1363 1364 1365 &
1366 1367 1368
nps  1e8
print
```

Appendix B.2- Primary Gamma Dose Profile Example (Truncated)

```
   Title
C CF-252 Gamma dose distribution in water phantom with default x-sec
C CELL CARDS
C source cell cards**************************************
2 0 1000 -2000 IMP:p,e=1 $ gap space
3 4 -21.53 2000 -3000 IMP:p,e=1 $ casing
4 3 -12 -1000 IMP:p,e=1 $ source
C 5 1 -1.0 3 -9999 IMP:p,e=1 $ water medium
9 0 9999 IMP:p,e=0 $ outside boundary
C top of source*******************************************
100 2 -1 101 -102  1  -2 imp:p,e=1
101 2 -1 101 -102  2  -3 imp:p,e=1
102 2 -1 101 -102  3  -4 imp:p,e=1
103 2 -1 101 -102  4  -5 imp:p,e=1
104 2 -1 101 -102  5  -6 imp:p,e=1
105 2 -1 101 -102  6  -7 imp:p,e=1
106 2 -1 101 -102  7  -8 imp:p,e=1
107 2 -1 101 -102  8  -9 imp:p,e=1
108 2 -1 101 -102  9 -10 imp:p,e=1
109 2 -1 101 -102 10 -11 imp:p,e=1
110 2 -1 101 -102 11 -12 imp:p,e=1
111 2 -1 101 -102 12 -13 imp:p,e=1
112 2 -1 101 -102 13 -14 imp:p,e=1
113 2 -1 101 -102 14 -15 imp:p,e=1
114 2 -1 101 -102 15 -16 imp:p,e=1
115 2 -1 101 -102 16 -17 imp:p,e=1
116 2 -1 101 -102 17 -18 imp:p,e=1
117 2 -1 101 -102 18 -19 imp:p,e=1
118 2 -1 101 -102 19 -20 imp:p,e=1
.
. condensed for space
.
1350 2 -1 126 -127  1  -2 imp:p,e=1
1351 2 -1 126 -127  2  -3 imp:p,e=1
1352 2 -1 126 -127  3  -4 imp:p,e=1
1353 2 -1 126 -127  4  -5 imp:p,e=1
1354 2 -1 126 -127  5  -6 imp:p,e=1
1355 2 -1 126 -127  6  -7 imp:p,e=1
1356 2 -1 126 -127  7  -8 imp:p,e=1
1357 2 -1 126 -127  8  -9 imp:p,e=1
1358 2 -1 126 -127  9 -10 imp:p,e=1
1359 2 -1 126 -127 10 -11 imp:p,e=1
1360 2 -1 126 -127 11 -12 imp:p,e=1
1361 2 -1 126 -127 12 -13 imp:p,e=1
1362 2 -1 126 -127 13 -14 imp:p,e=1
1363 2 -1 126 -127 14 -15 imp:p,e=1
1364 2 -1 126 -127 15 -16 imp:p,e=1
1365 2 -1 126 -127 16 -17 imp:p,e=1
1366 2 -1 126 -127 17 -18 imp:p,e=1
1367 2 -1 126 -127 18 -19 imp:p,e=1
```

1368 2 -1 126 -127 19 -20 imp:p,e=1
C end of shells **
8 2 -1.0 -9999 127 imp:p,e=1
10 2 -1.0 -9999 -127 -1 101 imp:p,e=1
11 2 -1.0 20 -9999 -127 101 imp:p,e=1
12 2 -1.0 -101 3000 -9999 imp:p,e=1

C SURFACE CARDS
C Source terms
1000 RCC 0 0 -.25 0 0 .5 .025 $ source
2000 RCC 0 0 -.38 0 0 .76 .035 $ gap
3000 RCC 0 0 -.4 0 0 .8 .055 $ casing
9999 RCC 0 0 -10 0 0 20 10 $ outside boundary h=20cm and r=10cm
C planes ********************************
1 PZ -.05
2 PZ .05
3 PZ .4
4 PZ .6
5 PZ .9
6 PZ 1.1
7 PZ 1.4
8 PZ 1.6
9 PZ 1.9
10 PZ 2.1
11 PZ 2.3
12 PZ 2.7
13 PZ 2.8
14 PZ 3.2
15 PZ 3.3
16 PZ 3.7
17 PZ 3.8
18 PZ 4.2
19 PZ 4.3
20 PZ 4.7 $ end planes
C cylinders ***************************
101 CZ .2825
102 CZ .3025
103 CZ .535
104 CZ .635
105 CZ .985
106 CZ 1.185
107 CZ 1.485
108 CZ 1.685
109 CZ 1.985
110 CZ 2.185
111 CZ 2.485
112 CZ 2.685
113 CZ 2.985
114 CZ 3.185
115 CZ 3.385
116 CZ 3.785
117 CZ 3.885
118 CZ 4.285
119 CZ 4.385
120 CZ 4.785

```
121 CZ 4.885
122 CZ 5.285
123 CZ 5.385
124 CZ 5.785
125 CZ 5.885
126 CZ 5.9
127 CZ 6.0 $ end shells

C MATERIALS
m2 1001 2 8016 1 $ water medium
C m3 46108 -2.5032 98252 -11.8556 8016 -1.1364 $ CF source
m3 46102 .01001 46104 .1103 46105 .2211 46106 .2706 46108 .2619 46110 .1160&
96248 .00727 98252 .00283
m4 77000 -10 78000 -90 $ Pt-10%Ir casing
SDEF ERG=D1 POS=0 0 0 CEL=4 RAD=D2 EXT=D3 AXS=0 0 1
C SI1 H .01 .05 .1 .2 .3 .4 .6 .8 1 1.33 1.66 2 2.5 3 4 5 6.5 8 10
C sp1 D 0 7.3e5 1.613e3 2.515e3 3.54e6 7.587e3 5.242e-1 3.073e6 5.63e-2
C 1.264e6 0 5.507e5 3.338e5 1.937e5 1.740e5 5.875e5 2.358e4 4.627e3 9.825e2
C probabilities from Cf-252 newsletter
SI1 H 0.01 0.0104 0.0107 0.0111 0.0115 0.0119 0.0124 0.0128 0.0133 0.0138&
0.0143 0.0148 0.0153 0.0159 0.0164 0.017 0.0177 0.0183 0.019 0.0196 0.0204&
0.0211 0.0219 0.0226 0.0235 0.0243 0.0252 0.0261 0.027 0.028 0.029 0.0301&
0.0312 0.0323 0.0335 0.0347 0.0359 0.0372 0.0386 0.04 0.0414 0.0429 0.0445&
0.0461 0.0478 0.0495 0.0513 0.0531 0.0551 0.0571 0.0591 0.0613 0.0635 0.0658&
0.0681 0.0706 0.0732 0.0758 0.0786 0.0814 0.0843 0.0874 0.0906 0.0938 0.0972&
0.101 0.104 0.108 0.112 0.116 0.12 0.125 0.129 0.134 0.139 0.144 0.149 0.154&
0.16 0.166 0.172 0.178 0.184 0.191 0.198 0.205 0.212 0.22 0.228 0.236 0.245&
0.254 0.263 0.273 0.282 0.293 0.303 0.314 0.325 0.337 0.349 0.362 0.375&
0.389 0.403 0.417 0.433 0.448 0.464 0.481 0.499 0.517 0.535 0.555 0.575&
0.596 0.617 0.639 0.663 0.687 0.711 0.737 0.764 0.791 0.82 0.85 0.88 0.912&
0.945 0.98 1.01 1.05 1.09 1.13 1.17 1.21 1.26 1.3 1.35 1.4 1.45 1.5 1.55&
1.61 1.67 1.73 1.79 1.86 1.92 1.99 2.07 2.14 2.22 2.3 2.38 2.47 2.56 2.65&
2.75 2.84 2.95 3.05 3.16 3.28 3.4 3.52 3.65 3.78 3.92 4.06 4.21 4.36 4.52&
4.68 4.85 5.02 5.2 5.39 5.59 5.79 6 6.21 6.42 6.63 6.84 7.05 7.26 7.47&
7.68 7.89 8.11 8.74 9.16 9.58 9.8
Sp1 D 0 1.01E-02 2.89E+01 6.79E+03 7.59E+00 2.45E+01 4.70E+01 5.55E+01&
2.02E+00 2.87E+02 1.38E+03 1.63E+00 1.19E+06 1.13E+03 1.13E+03 1.81E+03&
7.89E+03 1.55E+04 3.57E+04 1.03E+05 6.84E+03 3.58E+04 5.20E+03 1.74E+04&
2.70E+03 7.73E+03 3.89E+03 1.68E+03 2.17E+03 5.43E+03 1.71E+04 8.01E+03&
2.34E+04 1.72E+04 3.12E+04 9.76E+03 2.65E+04 4.79E+04 2.69E+04 1.57E+04&
2.63E+04 1.06E+04 1.03E+04 4.86E+03 1.39E+03 3.82E+03 1.17E+04 4.42E+02&
3.17E+03 1.11E+03 5.71E+03 2.50E+04 4.21E+03 1.47E+03 1.41E+03 2.93E+04&
7.49E+03 2.54E+03 6.61E+03 1.44E+04 5.34E+03 6.47E+03 3.34E+03 2.03E+04&
3.13E+03 1.41E+04 4.93E+04 1.49E+04 1.37E+04 1.41E+04 1.31E+04 2.52E+04&
3.81E+03 1.81E+04 2.87E+04 5.07E+04 2.21E+04 2.54E+05 2.31E+04 2.45E+04&
1.60E+04 2.17E+04 3.82E+04 2.68E+04 2.42E+04 1.43E+04 3.43E+04 2.67E+04&
3.72E+04 2.68E+04 2.55E+04 5.49E+05 6.71E+04 4.82E+04 3.64E+04 3.08E+04&
1.00E+05 5.68E+04 4.81E+04 5.66E+04 5.08E+04 6.67E+05 4.88E+04 5.48E+04&
5.97E+04 3.18E+04 5.92E+04 5.56E+04 6.21E+05 4.03E+04 7.39E+04 7.98E+04&
7.16E+04 6.31E+05 2.63E+04 6.71E+04 6.22E+04 6.62E+04 5.52E+05 4.88E+04&
5.88E+04 7.25E+04 3.40E+05 6.51E+04 5.53E+04 1.53E+05 1.25E+05 6.93E+04&
5.40E+04 2.48E+05 5.24E+04 1.89E+05 3.26E+04 3.80E+04 1.83E+05 3.51E+04&
1.05E+05 3.93E+04 1.18E+05 9.82E+04 5.87E+04 9.54E+04 7.11E+04 5.91E+04&
6.91E+04 2.34E+04 1.01E+05 8.18E+04 2.25E+04 6.14E+04 7.87E+04 2.19E+04&
6.45E+04 6.68E+04 5.33E+04 5.61E+04 5.23E+04 3.12E+04 3.30E+04 4.89E+04&
```

4.71E+04 3.77E+04 2.70E+04 2.36E+04 2.29E+04 1.59E+04 1.87E+04 6.73E+03&
1.13E+04 1.43E+04 7.35E+03 9.94E+03 5.90E+03 6.26E+03 4.68E+03 3.82E+03&
3.38E+03 2.47E+03 3.74E+03 1.70E+03 1.16E+03 1.16E+03 8.93E+02 7.96E+02&
4.64E+02 1.45E+02 1.41E+02 1.16E+02 5.21E+00 4.95E+00 9.30E-01 7.59E-01&
4.40E-01 2.55E-01 1.48E-01
C Gamma Spectrum using New ORIGEN LIBRARY
SI2 0 .024999
sp2 -21 0
SI3 -.24999 .24999
sp3 -21 0
*F8:P 100 101 102 103 104 105 106 107 108 109 110 111 &
112 113 114 115 116 117 118 150 151 152 153 154 155 156 &
157 158 159 160 161 162 163 164 165 166 167 168 ……..
.
. condensed for space
.
1300 1301 1302 1303 1304 1305 1306 1307 1308 1309 1310 &
1311 1312 1313 1314 1315 1316 1317 1318 1350 1351 1352 1353 &
1354 1355 1356 1357 1358 1359 1360 1361 1362 1363 1364 1365 &
1366 1367 1368
c
mode p e
nps 5e7
print

Appendix B.3- Secondary (n,γ) Dose Profile Example (Truncated)

Title
C CF-252 Secondary dose distribution in water phantom with default x-sec
C from Maxwellian fission spectrum
C   CELL CARDS
C source cell cards*************************************
2 0 1000 -2000   IMP:n,p,e=1 $ gap space
3 4 -21.53 2000 -3000 IMP:n,p,e=1 $ casing
4 3 -12 -1000 IMP:n,p,e=1 $ source
C 5 1 -1.0 3 -9999 IMP:n,p,e=1 $ water medium
9 0 9999   IMP:n,p,e=0 $ outside boundary
C top of source***
100 2 -1 101 -102 1 -2 imp:n,p,e=1
101 2 -1 101 -102 2 -3 imp:n,p,e=1
102 2 -1 101 -102 3 -4 imp:n,p,e=1
103 2 -1 101 -102 4 -5 imp:n,p,e=1
104 2 -1 101 -102 5 -6 imp:n,p,e=1
105 2 -1 101 -102 6 -7 imp:n,p,e=1
106 2 -1 101 -102 7 -8 imp:n,p,e=1
107 2 -1 101 -102 8 -9 imp:n,p,e=1
108 2 -1 101 -102 9 -10 imp:n,p,e=1
109 2 -1 101 -102 10 -11 imp:n,p,e=1
110 2 -1 101 -102 11 -12 imp:n,p,e=1
111 2 -1 101 -102 12 -13 imp:n,p,e=1
112 2 -1 101 -102 13 -14 imp:n,p,e=1
113 2 -1 101 -102 14 -15 imp:n,p,e=1
114 2 -1 101 -102 15 -16 imp:n,p,e=1
115 2 -1 101 -102 16 -17 imp:n,p,e=1
116 2 -1 101 -102 17 -18 imp:n,p,e=1
117 2 -1 101 -102 18 -19 imp:n,p,e=1
118 2 -1 101 -102 19 -20 imp:n,p,e=1
.
. condensed for space
.
1350 2 -1 126 -127 1 -2 imp:n,p,e=1
1351 2 -1 126 -127 2 -3 imp:n,p,e=1
1352 2 -1 126 -127 3 -4 imp:n,p,e=1
1353 2 -1 126 -127 4 -5 imp:n,p,e=1
1354 2 -1 126 -127 5 -6 imp:n,p,e=1
1355 2 -1 126 -127 6 -7 imp:n,p,e=1
1356 2 -1 126 -127 7 -8 imp:n,p,e=1
1357 2 -1 126 -127 8 -9 imp:n,p,e=1
1358 2 -1 126 -127 9 -10 imp:n,p,e=1
1359 2 -1 126 -127 10 -11 imp:n,p,e=1
1360 2 -1 126 -127 11 -12 imp:n,p,e=1
1361 2 -1 126 -127 12 -13 imp:n,p,e=1
1362 2 -1 126 -127 13 -14 imp:n,p,e=1
1363 2 -1 126 -127 14 -15 imp:n,p,e=1
1364 2 -1 126 -127 15 -16 imp:n,p,e=1
1365 2 -1 126 -127 16 -17 imp:n,p,e=1
1366 2 -1 126 -127 17 -18 imp:n,p,e=1

1367 2 -1 126 -127 18 -19 imp:n,p,e=1
1368 2 -1 126 -127 19 -20 imp:n,p,e=1
C end of shells **
8 2 -1.0 -9999 127   imp:n,p,e=1
10 2 -1.0 -9999 -127 -1 101 imp:n,p,e=1
11 2 -1.0 20 -9999 -127 101 imp:n,p,e=1
12 2 -1.0 -101 3000 -9999   imp:n,p,e=1

C SURFACE CARDS
C Source terms
1000 RCC 0 0 -.25 0 0 .5 .025 $ source
2000 RCC 0 0 -.38 0 0 .76 .035 $ gap
3000 RCC 0 0 -.4 0 0 .8 .055 $ casing
9999 RCC 0 0 -10 0 0 20 10 $ outside boundary h=20cm and r=10cm
C planes ********************************
1 PZ -.05
2 PZ .05
3 PZ .4
4 PZ .6
5 PZ .9
6 PZ 1.1
7 PZ 1.4
8 PZ 1.6
9 PZ 1.9
10 PZ 2.1
11 PZ 2.3
12 PZ 2.7
13 PZ 2.8
14 PZ 3.2
15 PZ 3.3
16 PZ 3.7
17 PZ 3.8
18 PZ 4.2
19 PZ 4.3
20 PZ 4.7 $ end planes
C cylinders ***************************
101 CZ .2825
102 CZ .3025
103 CZ .535
104 CZ .635
105 CZ .985
106 CZ 1.185
107 CZ 1.485
108 CZ 1.685
109 CZ 1.985
110 CZ 2.185
111 CZ 2.485
112 CZ 2.685
113 CZ 2.985
114 CZ 3.185
115 CZ 3.385
116 CZ 3.785
117 CZ 3.885
118 CZ 4.285
119 CZ 4.385

120 CZ 4.785
121 CZ 4.885
122 CZ 5.285
123 CZ 5.385
124 CZ 5.785
125 CZ 5.885
126 CZ 5.9
127 CZ 6.0 $ end shells

C MATERIALS
m2 1001 2 8016 1 $ water medium
mt2 lwtr.60
C m3 46108 -2.5032 98252 -11.8556 8016 -1.1364 CF source assumed to be all Pd
m3 46102 .01001 46104 .1103 46105 .2211 46106 .2706 46108 .2619 46110 .1160&
96248 .002423 98252 .00091 8016 .006667
m4 77000 -10 78000 -90 $ Pt-10%Ir casing
SDEF ERG=D1 POS=0 0 0 CEL=4 RAD=D2 EXT=D3 AXS=0 0 1
SP1 -2 1.42 $ maxwellian fission spectrum
SI2 0 .024999
sp2 -21 0
SI3 0.24999
sp3 -21 0
*F8:P 100 101 102 103 104 105 106 107 108 109 110 111 &
112 113 114 115 116 117 118 150 151 152 153 154 155 156 &
157 158 159 160 161 162 163 164 165 166 167 168 …….
.
. condensed for space
.
 1300 1301 1302 1303 1304 1305 1306 1307 1308 1309 1310 &
1311 1312 1313 1314 1315 1316 1317 1318 1350 1351 1352 1353 &
1354 1355 1356 1357 1358 1359 1360 1361 1362 1363 1364 1365 &
1366 1367 1368
mode n p e
nps 5e7
print

Appendix B.4- Bremsstrahlung Dose Profile Example (Truncated)

   Title
C CF-252 Gamma dose distribution in water phantom with default x-sec
C CELL CARDS
C source cell cards*************************************
2 0 1000 -2000 IMP:p,e=1 $ gap space
3 4 -21.53 2000 -3000 IMP:p,e=1 $ casing
4 3 -12 -1000 IMP:p,e=1 $ source
C 5 1 -1.0 3 -9999 IMP:p,e=1 $ water medium
9 0 9999 IMP:p,e=0 $ outside boundary
C top of source***
100 2 -1 101 -102 1 -2 imp:p,e=1
101 2 -1 101 -102 2 -3 imp:p,e=1
102 2 -1 101 -102 3 -4 imp:p,e=1
103 2 -1 101 -102 4 -5 imp:p,e=1
104 2 -1 101 -102 5 -6 imp:p,e=1
105 2 -1 101 -102 6 -7 imp:p,e=1
106 2 -1 101 -102 7 -8 imp:p,e=1
107 2 -1 101 -102 8 -9 imp:p,e=1
108 2 -1 101 -102 9 -10 imp:p,e=1
109 2 -1 101 -102 10 -11 imp:p,e=1
110 2 -1 101 -102 11 -12 imp:p,e=1
111 2 -1 101 -102 12 -13 imp:p,e=1
112 2 -1 101 -102 13 -14 imp:p,e=1
113 2 -1 101 -102 14 -15 imp:p,e=1
114 2 -1 101 -102 15 -16 imp:p,e=1
115 2 -1 101 -102 16 -17 imp:p,e=1
116 2 -1 101 -102 17 -18 imp:p,e=1
117 2 -1 101 -102 18 -19 imp:p,e=1
118 2 -1 101 -102 19 -20 imp:p,e=1
.
. condensed for space
.
1350 2 -1 126 -127 1 -2 imp:p,e=1
1351 2 -1 126 -127 2 -3 imp:p,e=1
1352 2 -1 126 -127 3 -4 imp:p,e=1
1353 2 -1 126 -127 4 -5 imp:p,e=1
1354 2 -1 126 -127 5 -6 imp:p,e=1
1355 2 -1 126 -127 6 -7 imp:p,e=1
1356 2 -1 126 -127 7 -8 imp:p,e=1
1357 2 -1 126 -127 8 -9 imp:p,e=1
1358 2 -1 126 -127 9 -10 imp:p,e=1
1359 2 -1 126 -127 10 -11 imp:p,e=1
1360 2 -1 126 -127 11 -12 imp:p,e=1
1361 2 -1 126 -127 12 -13 imp:p,e=1
1362 2 -1 126 -127 13 -14 imp:p,e=1
1363 2 -1 126 -127 14 -15 imp:p,e=1
1364 2 -1 126 -127 15 -16 imp:p,e=1
1365 2 -1 126 -127 16 -17 imp:p,e=1
1366 2 -1 126 -127 17 -18 imp:p,e=1
1367 2 -1 126 -127 18 -19 imp:p,e=1

1368 2 -1 126 -127 19 -20 imp:p,e=1
C end of shells **
8 2 -1.0 -9999 127 imp:p,e=1
10 2 -1.0 -9999 -127 -1 101 imp:p,e=1
11 2 -1.0 20 -9999 -127 101 imp:p,e=1
12 2 -1.0 -101 3000 -9999 imp:p,e=1

C SURFACE CARDS
C Source terms
1000 RCC 0 0 -.25 0 0 .5 .025 $ source
2000 RCC 0 0 -.38 0 0 .76 .035 $ gap
3000 RCC 0 0 -.4 0 0 .8 .055 $ casing
9999 RCC 0 0 -10 0 0 20 10 $ outside boundary h=20cm and r=10cm
C planes *********************************
1 PZ -.05
2 PZ .05
3 PZ .4
4 PZ .6
5 PZ .9
6 PZ 1.1
7 PZ 1.4
8 PZ 1.6
9 PZ 1.9
10 PZ 2.1
11 PZ 2.3
12 PZ 2.7
13 PZ 2.8
14 PZ 3.2
15 PZ 3.3
16 PZ 3.7
17 PZ 3.8
18 PZ 4.2
19 PZ 4.3
20 PZ 4.7 $ end planes
C cylinders ***************************
101 CZ .2825
102 CZ .3025
103 CZ .535
104 CZ .635
105 CZ .985
106 CZ 1.185
107 CZ 1.485
108 CZ 1.685
109 CZ 1.985
110 CZ 2.185
111 CZ 2.485
112 CZ 2.685
113 CZ 2.985
114 CZ 3.185
115 CZ 3.385
116 CZ 3.785
117 CZ 3.885
118 CZ 4.285
119 CZ 4.385
120 CZ 4.785

```
121 CZ 4.885
122 CZ 5.285
123 CZ 5.385
124 CZ 5.785
125 CZ 5.885
126 CZ 5.9
127 CZ 6.0 $ end shells

C MATERIALS
m2 1001 2 8016 1 $ water medium
C m3 46108 -2.5032 98252 -11.8556 8016 -1.1364 $ CF source
m3 46102 .01001 46104 .1103 46105 .2211 46106 .2706 46108 .2619 46110 .1160&
96248 .00727 98252 .00283
m4 77000 -10 78000 -90 $ Pt-10%Ir casing
SDEF ERG=D1 POS=0 0 0 CEL=4 RAD=D2 EXT=D3 AXS=0 0 1 PAR=3
C SI1 H .01 .05 .1 .2 .3 .4 .6 .8 1 1.33 1.66 2 2.5 3 4 5 6.5 8 10
C sp1 D 0 7.3e5 1.613e3 2.515e3 3.54e6 7.587e3 5.242e-1 3.073e6 5.63e-2
C 1.264e6 0 5.507e5 3.338e5 1.937e5 1.740e5 5.875e5 2.358e4 4.627e3 9.825e2
C probabilities from Cf-252 newsletter
SI1 H 0.000 0.025 0.050 0.075 0.100 0.125 0.150 0.175 0.200 0.225 0.250 0.275&
0.300 0.325 0.350 0.375 0.400 0.425 0.450 0.475 0.500 0.525 0.550 0.575 0.600&
0.625 0.650 0.675 0.700 0.725 0.750 0.775 0.800 0.825 0.850 0.875 0.900 0.925&
0.950 0.975 1.000 1.020 1.050 1.070 1.100 1.120 1.150 1.170 1.200 1.220 1.250&
1.270 1.300 1.320 1.350 1.370 1.400 1.420 1.450 1.470 1.500 1.520 1.550 1.570&
1.600 1.620 1.650 1.670 1.700 1.720 1.750 1.770 1.800 1.820 1.850 1.870 1.900&
1.920 1.950 1.970 2.000 2.020 2.050 2.070 2.100 2.120 2.150 2.170 2.200 2.220&
2.250 2.270 2.300 2.320 2.350 2.380 2.400 2.420 2.450 2.470 2.500 2.520 2.550&
2.570 2.600 2.620 2.650 2.670 2.700 2.720 2.750 2.770 2.800 2.820 2.850 2.880&
2.900 2.920 2.950 2.970 3.000 3.020 3.050 3.070 3.100 3.120 3.150 3.170 3.200&
3.220 3.250 3.270 3.300 3.330 3.350 3.380 3.400 3.420 3.450 3.470 3.500 3.520&
3.550 3.580 3.600 3.620 3.650 3.670 3.700 3.720 3.750 3.770 3.800 3.830 3.850&
3.880 3.900 3.920 3.950 3.970 4.000 4.030 4.050 4.070 4.100 4.120 4.150 4.170&
4.200 4.220 4.250 4.280 4.300 4.320 4.350 4.380 4.400 4.420 4.450 4.470 4.500&
4.530 4.550 4.570 4.600 4.620 4.650 4.670 4.700 4.720 4.750 4.780 4.800 4.820&
4.850 4.880 4.900 4.930 4.950 4.970 5.000 5.030 5.050 5.070 5.100 5.120 5.150&
5.180 5.200 5.220 5.250 5.280 5.300 5.320 5.350 5.380 5.400 5.430 5.450 5.470&
5.500 5.530 5.550 5.570 5.600 5.620 5.650 5.680 5.700 5.720 5.750 5.780 5.800&
5.820 5.850 5.880 5.900 5.930 5.950 5.970 6.000 6.030 6.050 6.070 6.100 6.120&
6.150 6.180 6.200 6.220 6.250 6.280 6.300 6.320 6.350 6.380 6.400 6.430 6.450&
6.470 6.500 6.530 6.550 6.570 6.600 6.620 6.650 6.680 6.700 6.720 6.750 6.780&
6.800 6.820 6.850 6.880 6.900 6.930 6.950 6.970 7.000 7.030 7.050 7.070 7.100&
7.120 7.150 7.180 7.200 7.220 7.250 7.280 7.300 7.320 7.350 7.380 7.400 7.430&
7.450 7.470 7.500 7.530 7.550 7.570 7.600 7.620 7.650 7.680 7.700 7.720 7.750&
7.780 7.800 7.820 7.850 7.880 7.900 7.930 7.950 7.970 8.000
Sp1 D 0 8.48E+05 8.70E+04 7.87E+04 7.32E+04 6.80E+04 6.32E+04 5.91E+04&
5.57E+04 5.32E+04 5.15E+04 5.00E+04 4.87E+04 4.74E+04 4.63E+04 4.53E+04&
4.42E+04 4.32E+04 4.22E+04 4.13E+04 4.04E+04 3.95E+04 3.86E+04 3.78E+04&
3.70E+04 3.62E+04 3.54E+04 3.46E+04 3.39E+04 3.31E+04 3.24E+04 3.17E+04&
3.09E+04 3.02E+04 2.95E+04 2.89E+04 2.82E+04 2.76E+04 2.70E+04 2.65E+04&
2.59E+04 2.55E+04 2.50E+04 2.46E+04 2.42E+04 2.38E+04 2.34E+04 2.31E+04&
2.27E+04 2.24E+04 2.20E+04 2.17E+04 2.14E+04 2.10E+04 2.07E+04 2.04E+04&
2.01E+04 1.98E+04 1.95E+04 1.91E+04 1.88E+04 1.85E+04 1.82E+04 1.79E+04&
1.76E+04 1.73E+04 1.69E+04 1.66E+04 1.63E+04 1.60E+04 1.57E+04 1.54E+04&
1.51E+04 1.49E+04 1.46E+04 1.43E+04 1.40E+04 1.37E+04 1.35E+04 1.32E+04&
1.29E+04 1.27E+04 1.24E+04 1.22E+04 1.20E+04 1.17E+04 1.15E+04 1.13E+04&
```

```
1.10E+04 1.08E+04 1.06E+04 1.04E+04 1.02E+04 1.00E+04 9.79E+03 9.59E+03&
9.39E+03 9.20E+03 9.00E+03 8.82E+03 8.63E+03 8.44E+03 8.26E+03 8.08E+03&
7.90E+03 7.73E+03 7.55E+03 7.38E+03 7.22E+03 7.05E+03 6.89E+03 6.73E+03&
6.57E+03 6.42E+03 6.27E+03 6.13E+03 5.98E+03 5.84E+03 5.71E+03 5.57E+03&
5.44E+03 5.31E+03 5.19E+03 5.07E+03 4.95E+03 4.83E+03 4.72E+03 4.60E+03&
4.49E+03 4.38E+03 4.28E+03 4.18E+03 4.08E+03 3.98E+03 3.89E+03 3.80E+03&
3.71E+03 3.62E+03 3.53E+03 3.45E+03 3.36E+03 3.28E+03 3.20E+03 3.12E+03&
3.04E+03 2.96E+03 2.89E+03 2.81E+03 2.73E+03 2.66E+03 2.59E+03 2.52E+03&
2.45E+03 2.38E+03 2.31E+03 2.24E+03 2.18E+03 2.11E+03 2.05E+03 1.99E+03&
1.93E+03 1.87E+03 1.82E+03 1.76E+03 1.71E+03 1.66E+03 1.61E+03 1.56E+03&
1.51E+03 1.46E+03 1.42E+03 1.38E+03 1.33E+03 1.29E+03 1.25E+03 1.22E+03&
1.18E+03 1.14E+03 1.11E+03 1.08E+03 1.04E+03 1.01E+03 9.83E+02 9.55E+02&
9.27E+02 8.99E+02 8.72E+02 8.47E+02 8.22E+02 7.97E+02 7.73E+02 7.50E+02&
7.27E+02 7.06E+02 6.84E+02 6.63E+02 6.42E+02 6.23E+02 6.04E+02 5.85E+02&
5.67E+02 5.50E+02 5.33E+02 5.16E+02 5.00E+02 4.84E+02 4.69E+02 4.55E+02&
4.40E+02 4.27E+02 4.13E+02 4.00E+02 3.87E+02 3.75E+02 3.63E+02 3.51E+02&
3.40E+02 3.29E+02 3.18E+02 3.07E+02 2.97E+02 2.87E+02 2.78E+02 2.68E+02&
2.59E+02 2.50E+02 2.42E+02 2.34E+02 2.25E+02 2.18E+02 2.10E+02 2.03E+02&
1.96E+02 1.89E+02 1.82E+02 1.75E+02 1.69E+02 1.63E+02 1.57E+02 1.51E+02&
1.46E+02 1.40E+02 1.35E+02 1.30E+02 1.25E+02 1.21E+02 1.16E+02 1.12E+02&
1.07E+02 1.03E+02 9.95E+01 9.58E+01 9.23E+01 8.88E+01 8.54E+01 8.22E+01&
7.90E+01 7.59E+01 7.30E+01 7.01E+01 6.73E+01 6.46E+01 6.21E+01 5.96E+01&
5.72E+01 5.49E+01 5.27E+01 5.06E+01 4.85E+01 4.65E+01 4.45E+01 4.27E+01&
4.08E+01 3.91E+01 3.74E+01 3.57E+01 3.41E+01 3.26E+01 3.11E+01 2.97E+01&
2.83E+01 2.70E+01 2.58E+01 2.46E+01 2.34E+01 2.24E+01 2.13E+01 2.03E+01&
1.94E+01 1.85E+01 1.76E+01 1.68E+01 1.61E+01 1.53E+01 1.47E+01 1.41E+01&
1.34E+01 1.29E+01 1.23E+01 1.18E+01 1.13E+01 1.08E+01 1.04E+01 9.93E+00&
9.50E+00 9.08E+00 8.68E+00 8.30E+00 7.93E+00 7.58E+00 7.24E+00 6.92E+00&
6.61E+00 6.32E+00 6.04E+00 5.78E+00 5.53E+00 5.28E+00 5.05E+00 4.83E+00&
4.62E+00
C Gamma Spectrum using New ORIGEN LIBRARY
SI2 0 .024999
sp2 -21 0
SI3 -.24999 .24999
sp3 -21 0
*F8:P 100 101 102 103 104 105 106 107 108 109 110 111 &
112 113 114 115 116 117 118 150 151 152 153 154 155 156 &
157 158 159 160 161 162 163 164 165 166 167 168…..
.
. condensed for space
.
1300 1301 1302 1303 1304 1305 1306 1307 1308 1309 1310 &
1311 1312 1313 1314 1315 1316 1317 1318 1350 1351 1352 1353 &
1354 1355 1356 1357 1358 1359 1360 1361 1362 1363 1364 1365 &
1366 1367 1368
c
mode p e
nps 3e7
print
```

Appendix B.5- Leakage Spectrum MCNP Input Example (Truncated)

```
   Title
C CF-252 Gamma dose distribution in water phantom with default x-sec
C CELL CARDS
C source cell cards*************************************
2 0 1000 -2000 IMP:p,e=1 $ gap space
3 4 -21.53 2000 -3000 IMP:p,e=1 $ casing
4 3 -12 -1000 IMP:p,e=1 $ source
5 2 -1.0 3000 -4000 IMP:p,e=1 $ Surface Tally
C 5 1 -1.0 3 -9999 IMP:p,e=1 $ water medium
9 0 9999 IMP:p,e=0 $ outside boundary
C top of source*********************************************
100 2 -1 101 -102  1  -2 imp:p,e=1
101 2 -1 101 -102  2  -3 imp:p,e=1
102 2 -1 101 -102  3  -4 imp:p,e=1
103 2 -1 101 -102  4  -5 imp:p,e=1
104 2 -1 101 -102  5  -6 imp:p,e=1
105 2 -1 101 -102  6  -7 imp:p,e=1
106 2 -1 101 -102  7  -8 imp:p,e=1
107 2 -1 101 -102  8  -9 imp:p,e=1
108 2 -1 101 -102  9 -10 imp:p,e=1
109 2 -1 101 -102 10 -11 imp:p,e=1
110 2 -1 101 -102 11 -12 imp:p,e=1
111 2 -1 101 -102 12 -13 imp:p,e=1
112 2 -1 101 -102 13 -14 imp:p,e=1
113 2 -1 101 -102 14 -15 imp:p,e=1
114 2 -1 101 -102 15 -16 imp:p,e=1
115 2 -1 101 -102 16 -17 imp:p,e=1
116 2 -1 101 -102 17 -18 imp:p,e=1
117 2 -1 101 -102 18 -19 imp:p,e=1
118 2 -1 101 -102 19 -20 imp:p,e=1
.
. condensed for space
.
1350 2 -1 126 -127  1  -2 imp:p,e=1
1351 2 -1 126 -127  2  -3 imp:p,e=1
1352 2 -1 126 -127  3  -4 imp:p,e=1
1353 2 -1 126 -127  4  -5 imp:p,e=1
1354 2 -1 126 -127  5  -6 imp:p,e=1
1355 2 -1 126 -127  6  -7 imp:p,e=1
1356 2 -1 126 -127  7  -8 imp:p,e=1
1357 2 -1 126 -127  8  -9 imp:p,e=1
1358 2 -1 126 -127  9 -10 imp:p,e=1
1359 2 -1 126 -127 10 -11 imp:p,e=1
1360 2 -1 126 -127 11 -12 imp:p,e=1
1361 2 -1 126 -127 12 -13 imp:p,e=1
1362 2 -1 126 -127 13 -14 imp:p,e=1
1363 2 -1 126 -127 14 -15 imp:p,e=1
1364 2 -1 126 -127 15 -16 imp:p,e=1
1365 2 -1 126 -127 16 -17 imp:p,e=1
1366 2 -1 126 -127 17 -18 imp:p,e=1
```

1367 2 -1 126 -127 18 -19 imp:p,e=1
1368 2 -1 126 -127 19 -20 imp:p,e=1
C end of shells **
8 2 -1.0 -9999 127 imp:p,e=1
10 2 -1.0 -9999 -127 -1 101 imp:p,e=1
11 2 -1.0 20 -9999 -127 101 imp:p,e=1
12 2 -1.0 -101 4000 -9999 imp:p,e=1

C SURFACE CARDS
C Source terms
1000 RCC 0 0 -.25 0 0 .5 .025 $ source
2000 RCC 0 0 -.38 0 0 .76 .035 $ gap
3000 RCC 0 0 -.4 0 0 .8 .055 $ casing
4000 RCC 0 0 -1 0 0 2 .056 $surface tally
9999 RCC 0 0 -10 0 0 20 10 $ outside boundary h=20cm and r=10cm
C planes ***********************************
1 PZ -.05
2 PZ .05
3 PZ .4
4 PZ .6
5 PZ .9
6 PZ 1.1
7 PZ 1.4
8 PZ 1.6
9 PZ 1.9
10 PZ 2.1
11 PZ 2.3
12 PZ 2.7
13 PZ 2.8
14 PZ 3.2
15 PZ 3.3
16 PZ 3.7
17 PZ 3.8
18 PZ 4.2
19 PZ 4.3
20 PZ 4.7 $ end planes
C cylinders **************************
101 CZ .2825
102 CZ .3025
103 CZ .535
104 CZ .635
105 CZ .985
106 CZ 1.185
107 CZ 1.485
108 CZ 1.685
109 CZ 1.985
110 CZ 2.185
111 CZ 2.485
112 CZ 2.685
113 CZ 2.985
114 CZ 3.185
115 CZ 3.385
116 CZ 3.785
117 CZ 3.885
118 CZ 4.285

119 CZ 4.385
120 CZ 4.785
121 CZ 4.885
122 CZ 5.285
123 CZ 5.385
124 CZ 5.785
125 CZ 5.885
126 CZ 5.9
127 CZ 6.0 $ end shells

C MATERIALS
m2 1001 2 8016 1 $ water medium
C m3 46108 -2.5032 98252 -11.8556 8016 -1.1364 $ CF source
m3 46102 .01001 46104 .1103 46105 .2211 46106 .2706 46108 .2619 46110 .1160&
96248 .00727 98252 .00283
m4 77000 -10 78000 -90 $ Pt-10%Ir casing
SDEF ERG=D1 POS=0 0 0 CEL=4 RAD=D2 EXT=D3 AXS=0 0 1
C SI1 H .01 .05 .1 .2 .3 .4 .6 .8 1 1.33 1.66 2 2.5 3 4 5 6.5 8 10
C sp1 D 0 7.3e5 1.613e3 2.515e3 3.54e6 7.587e3 5.242e-1 3.073e6 5.63e-2
C 1.264e6 0 5.507e5 3.338e5 1.937e5 1.740e5 5.875e5 2.358e4 4.627e3 9.825e2
C probabilities from Cf-252 newsletter
SI1 H 0.01 0.0104 0.0107 0.0111 0.0115 0.0119 0.0124 0.0128 0.0133 0.0138&
0.0143 0.0148 0.0153 0.0159 0.0164 0.017 0.0177 0.0183 0.019 0.0196 0.0204&
0.0211 0.0219 0.0226 0.0235 0.0243 0.0252 0.0261 0.027 0.028 0.029 0.0301&
0.0312 0.0323 0.0335 0.0347 0.0359 0.0372 0.0386 0.04 0.0414 0.0429 0.0445&
0.0461 0.0478 0.0495 0.0513 0.0531 0.0551 0.0571 0.0591 0.0613 0.0635 0.0658&
0.0681 0.0706 0.0732 0.0758 0.0786 0.0814 0.0843 0.0874 0.0906 0.0938 0.0972&
0.101 0.104 0.108 0.112 0.116 0.12 0.125 0.129 0.134 0.139 0.144 0.149 0.154&
0.16 0.166 0.172 0.178 0.184 0.191 0.198 0.205 0.212 0.22 0.228 0.236 0.245&
0.254 0.263 0.273 0.282 0.293 0.303 0.314 0.325 0.337 0.349 0.362 0.375&
0.389 0.403 0.417 0.433 0.448 0.464 0.481 0.499 0.517 0.535 0.555 0.575&
0.596 0.617 0.639 0.663 0.687 0.711 0.737 0.764 0.791 0.82 0.85 0.88 0.912&
0.945 0.98 1.01 1.05 1.09 1.13 1.17 1.21 1.26 1.3 1.35 1.4 1.45 1.5 1.55&
1.61 1.67 1.73 1.79 1.86 1.92 1.99 2.07 2.14 2.22 2.3 2.38 2.47 2.56 2.65&
2.75 2.84 2.95 3.05 3.16 3.28 3.4 3.52 3.65 3.78 3.92 4.06 4.21 4.36 4.52&
4.68 4.85 5.02 5.2 5.39 5.59 5.79 6 6.21 6.42 6.63 6.84 7.05 7.26 7.47&
7.68 7.89 8.11 8.74 9.16 9.58 9.8
Sp1 D 0 1.01E-02 2.89E+01 6.79E+03 7.59E+00 2.45E+01 4.70E+01 5.55E+01&
2.02E+00 2.87E+02 1.38E+03 1.63E+00 1.19E+06 1.13E+03 1.13E+03 1.81E+03&
7.89E+03 1.55E+04 3.57E+04 1.03E+05 6.84E+03 3.58E+04 5.20E+03 1.74E+04&
2.70E+03 7.73E+03 3.89E+03 1.68E+03 2.17E+03 5.43E+03 1.71E+04 8.01E+03&
2.34E+04 1.72E+04 3.12E+04 9.76E+03 2.65E+04 4.79E+04 2.69E+04 1.57E+04&
2.63E+04 1.06E+04 1.03E+04 4.86E+03 1.39E+03 3.82E+03 1.17E+04 4.42E+02&
3.17E+03 1.11E+03 5.71E+03 2.50E+04 4.21E+03 1.47E+03 1.41E+03 2.93E+04&
7.49E+03 2.54E+03 6.61E+03 1.44E+04 5.34E+03 6.47E+03 3.34E+03 2.03E+04&
3.13E+03 1.41E+04 4.93E+04 1.49E+04 1.37E+04 1.41E+04 1.31E+04 2.52E+04&
3.81E+03 1.81E+04 2.87E+04 5.07E+04 2.21E+04 2.54E+05 2.31E+04 2.45E+04&
1.60E+04 2.17E+04 3.82E+04 2.68E+04 2.42E+04 1.43E+04 3.43E+04 2.67E+04&
3.72E+04 2.68E+04 2.55E+04 5.49E+05 6.71E+04 4.82E+04 3.64E+04 3.08E+04&
1.00E+05 5.68E+04 4.81E+04 5.66E+04 5.08E+04 6.67E+05 4.88E+04 5.48E+04&
5.97E+04 3.18E+04 5.92E+04 5.56E+04 6.21E+05 4.03E+04 7.39E+04 7.98E+04&
7.16E+04 6.31E+05 2.63E+04 6.71E+04 6.22E+04 6.62E+04 5.52E+05 4.88E+04&
5.88E+04 7.25E+04 3.40E+05 6.51E+04 5.53E+04 1.53E+05 1.25E+05 6.93E+04&
5.40E+04 2.48E+05 5.24E+04 1.89E+05 3.26E+04 3.80E+04 1.83E+05 3.51E+04&
1.05E+05 3.93E+04 1.18E+05 9.82E+04 5.87E+04 9.54E+04 7.11E+04 5.91E+04&

6.91E+04 2.34E+04 1.01E+05 8.18E+04 2.25E+04 6.14E+04 7.87E+04 2.19E+04&
6.45E+04 6.68E+04 5.33E+04 5.61E+04 5.23E+04 3.12E+04 3.30E+04 4.89E+04&
4.71E+04 3.77E+04 2.70E+04 2.36E+04 2.29E+04 1.59E+04 1.87E+04 6.73E+03&
1.13E+04 1.43E+04 7.35E+03 9.94E+03 5.90E+03 6.26E+03 4.68E+03 3.82E+03&
3.38E+03 2.47E+03 3.74E+03 1.70E+03 1.16E+03 1.16E+03 8.93E+02 7.96E+02&
4.64E+02 1.45E+02 1.41E+02 1.16E+02 5.21E+00 4.95E+00 9.30E-01 7.59E-01&
4.40E-01 2.55E-01 1.48E-01
C Gamma Spectrum using New ORIGEN LIBRARY
SI2 0 .024999
sp2 -21 0
SI3 -.24999 .24999
sp3 -21 0
F1:P 4000.1
sd2 .70372
e0 0.03 0.06 0.09 0.12 0.15 0.18 0.21 0.24 0.27 0.3 0.33 0.36 0.39 0.42 0.45&
0.48 0.51 0.54 0.57 0.6 0.63 0.66 0.69 0.72 0.75 0.78 0.81 0.84 0.87 0.9&
0.95 1.1 1.2 1.3 1.4 1.5 1.6 1.7 1.8 1.9 2.0 2.5 3.0 3.5 4.0 4.5 5.0 5.5&
6.0 6.6
c
mode p e
nps 5e7
print

51

REFERENCES

1. Stoddard, D.H. Historical Review of Californium-252 Discovery and Development. *Nucl Sci. Appl.* **2,** pp. 189-199,1986.

2. Wambersie, A. (Eds). *Fast Neutrons and High-LET Particles in Cancer Therapy.* Springer, 1998.

3. Vtyurin B.M. and Tsyb A.F. Brachytherapy with Cf-252 in USSR: Head and Neck, GYN, and Other Tumors. *Nucl. Sci. Appl.* **2,** pp. 521-538, 1986.

4. Maruyama, Y. et al Cf-252 Neutron Brachytherapy Treatment for Cure of Cervical Cancer. *Nuclear Science Applications,* **Vol. 4,** pp. 181-192, 1991.

5. Maruyama Y. et al Californium-252 Neutron Brachytherapy. Chapter 35 of *Principles and Practice of Brachytherapy*, Futura Publishing Co. Inc., Armonk, NY, 1997

6. ORNL Invention Disclosure No. 1289, under Cooperative Research and Development Agreement (CRADA) contract with Isotron Inc., 2002

7. Kelm, Robert S. *In-Water Neutron and Gamma Dose Determination for a New Cf-252 Brachytherapy Source*. MS Thesis. Georgia Institute of Technology, Atlanta, Ga. 2009.

8. X-5 Monte Carlo Team, MCNP- A General Monte Carlo N-Particle Transport Code Version 5, Los Alamos report LA-UR-03-1987, 2003.

9. Martin, R.C. Californium-252 Newsletter, 4, 1 Oak Ridge National Laboratory, January 2000.

10. Rivard, M.J "Dosimetry for ^{252}Cf Neutron Emitting Brachytherapy Source: Protocol, Measurements, and Calculations", Med. Phys, Vol. 26 (8), pp. 1503-1514, 1999.

11. Attix, F. H. *Introduction to Radiological Physics and Radiation Dosimetry*, pp 475-480, John Wiley & Sons, Inc., 1986.

12. Neutron Source Strength Calibration Report, NIST Test Number: 278144, Service ID: 44010C (June 2,2009)

13. SCALE: A Modular Code System for Performing Standardized Computer Analyses for Licensing Evaluation. ORNL/TM-2005/39, Version 5.1, Vols. I-III, Nov. 2006

14. Croft, A.G., Grove, N.B., Haese, R.L., *Updated Decay and Photon Libraries for the ORIGEN Code,* ORNL/TM-6055, Union Carbide Corporation (Nuclear Division), Oak Ridge National Laboratory, February 1979.

15. Verbinski, V.V., Weber, H., Sund, R.E., 1973. *Prompt Gamma Rays from ^{235}U (n,f), $^{239}Pu(n,f)$ and Spontaneous Fission of $^{252}Cf.$* Physics Review C7 (3), 1173-1185.

16. DigXY, Code System to Digitize and Extract Data from a Graph or Chart, Thunderhead Engineering Consultants 2003.

17. BETA-S 6.0, Code System to Calculate Multigroup Beta-Ray Spectra, Radiation Safety Information and Code Center package CCC-657.